NASA CR-54289

DEVELOPMENT OF A HIGH TEMPERATURE BATTERY

by

W.J. Subcasky, D.N. Stamires, T.M. Place, G. Segovia,
R.G. Salisbury, and A. Parker-Jones

prepared for

NATIONAL AERONAUTICS AND SPACE ADMINISTRATION

CONTRACT NAS3-6002

AERONUTRONIC
DIVISION OF PHILCO CORPORATION
A SUBSIDIARY OF Ford Motor Company
FORD ROAD/NEWPORT BEACH, CALIFORNIA

NASA CR 54289
Aeronutronic Publication No. U-2986
W.O. 2261

SECOND QUARTERLY TECHNICAL REPORT

DEVELOPMENT OF A HIGH TEMPERATURE BATTERY

by

W. J. Subcasky, D. N. Stamires, T. M. Place, G. Segovia,
R. G. Salisbury, and A. Parker-Jones

prepared for

NATIONAL AERONAUTICS AND SPACE ADMINISTRATION

January 15, 1965

Technical Management
NASA Lewis Research Center
Cleveland, Ohio
Space Power Systems Division
Meyer R. Unger

APPLIED RESEARCH LABORATORY
Aeronutronic Division
Philco Corporation
Newport Beach, California

OBJECTIVE

The objective of this program is to develop a high energy density battery capable of operation for three days at 800°F (424°C) in an environment approximately the same as exists on the planet Venus. The battery should also be capable of activation within less than ten minutes after exposure to 800°F temperature. The battery will be able to supply power to an instrument package in the Venus environment.

A thin synthetic zeolite membrane will be used to separate the anode and cathode section of the battery. The zeolite, acting as a solid electrolyte permeable only to cations, will eliminate many of the problems associated with the solubility and reactivity of materials in high temperature battery systems. The zeolite membrane will permit the use of high energy density components to produce a light weight battery.

SUMMARY

15882

The resistivities of various types of synthetic zeolites having different cations have been measured as a function of temperature. Of the materials NaX has the lowest resistance. The effect of various bonding techniques upon the crystal structure and resistivities of sodium zeolites was investigated. Techniques using $Na_2Si_2O_5$ or H_3PO_4 as a binding agent show increased resistances when compared to the pure zeolites.

The electrochemical characteristics of $CuCl_2$, $CuCl$, $BiCl_3$, $FeCl_3$, and AgCl are presented. The effect of diluents added as solids or coulometrically by cationic transfer through a ceramic membrane upon the performance of certain cathode materials was investigated.

Sodium was proposed as the anode material after elimination of calcium because of contact problems and lithium because of severe corrosion problems.

A proposed cell design is presented utilizing various sealing and containing techniques. Compatibility tests with materials of the proposed cell were initiated and used to further define the proposed cell.

AUTHOR

CONTENTS

ILLUSTRATIONS

TABLES

Page ___ Missing in Original Document

SECTION I

ZEOLITE STUDIES

In the proposed battery solid zeolite membranes will be used to separate the materials of the anode and cathode and to prevent their direct chemical reaction. During the second quarter efforts in the area of zeolite studies were directed towards the preparation of various zeolite types with different cations and the determination of their thermal stability and electrolytic resistance. In addition various zeolites were prepared for use in a possible solid state battery as proposed in the First Quarterly Report(1). During this period efforts were also initiated in better methods of fabricating thin zeolite membranes.

1.1 PREPARATION OF CRYSTALLINE ZEOLITES

The Type A and Type X zeolite powders are commercially available in both the Na^{+} and Ca^{++} forms. These commercially available A and X zeolites were used as the starting material for the studies with A and X zeolites. Type Y zeolite is not readily available and was therefore synthesized by crystallization from aluminosilicate gels. This preparation is given in detail in the next section.

1.1.1 PREPARATION OF TYPE Y SODIUM ZEOLITE

Dissolve 5.0 grams of $NaAlO_2$ (Matheson, Coleman, and Bell, Technical, CB941) and 22.0 grams of NaOH (Baker Analyzed Reagent, 3726) in 89.5 ml. of distilled water. Allow this solution to cool somewhat (actual temperature did not appear to be critical). Weigh out 125 grams of colloidal SiO_2 (Matheson, Coleman, and Bell, Practical, 30% SiO_2 by weight, P7694) and mix with $NaAlO_2$-NaOH solution in a Waring type blender until homogeneous.

Place the resultant paste in a 500 ml Erlenmeyer flask. Equip the flask with a reflux condenser and heat on a water bath for approximately 24 hours. During this period, the homogeneous gel recrystallizes into an easily separable solid phase. The solid phase is removed by vacuum filtration and washed with distilled water until the pH of the filtrate drops to about 10.5. Four 50 ml portions of distilled water are usually sufficient. Occasionally this method of preparation produced a batch in which the washings remain at pH 12. This material was always found to be amorphous to X-rays.

After filtering and washing, the solid is air dried overnight or for several hours at 100°C. The zeolite can be activated (water removed from the pores) by vacuum drying at approximately 350°C. This preparation yields about 8 grams of the air dried but unactivated zeolite.

X-ray diffraction patterns indicated that the sodium form of type Y zeolite could be prepared. Several attempts to directly synthesize the lithium and potassium forms of type Y yield a material which was amorphous to X-rays. The lithium form of Type Y was therefore prepared by exchanging NaY with an aqueous solution of LiCl. Similarly, other cation forms of Type A and X zeolites were prepared by ion exchange of the sodium forms with the appropriate cation.

1.1.2 ZEOLITE ION EXCHANGE PROCEDURES

Several procedures were used to achieve ion exchange with the various cations and zeolite types.

A suspension of 0.1 equivalent of zeolite (based on replaceable cations) in the sodium form in 100 ml of a solution containing 0.1 equivalent of the exchanging cation was maintained at room temperature for approximately 0.5 hours by magnetic stirring. The solid was then removed by vacuum filtration. The suspension and filtration of zeolite was repeated until it had been exposed to a total of at least 0.3 equivalents of exchanging cations. After the final filtration, the zeolite was washed with a small portion of distilled water before drying at 100°C. in air and activating in vacuum at 350°C.

It was soon noted that the Teflon covered stirring bar was being abraded by this process and that the zeolite was being contaminated by material from the magnetic stirring bar. The procedure was modified by using a stream of air bubbling through the suspension instead of the magnetic stirring.

To achieve a greater degree of exchange a percolating procedure was devised. The zeolite to be exchanged was placed in a glass tube similar to a chromocographic column. Vacuum was applied at the base of the tube and a solution of the exchanging cation was allowed to percolate through the zeolite. The column was maintained at approximately 80°C. As in the preceding process, the zeolite was treated with a three fold excess of exchanging cation.

Generally, one normal aqueous solutions of the exchanging cations as nitrates or chlorides were used. Small amounts of acids were used to prevent hydrolysis of some of the salts. Type A and Type X zeolites are quite sensitive to acids and therefore the pH of the exchanging solutions was kept as high as possible. Type Z zeolite appeared to be decomposed by aqueous cupric solutions. Type A zeolite was exchanged using a one normal solution of $Cu(NO_3)_2 \cdot 3H_2O$ in 95% ethanol. A filterable blue solid was obtained. In drying and activating this material the temperature was kept below 150°C. At approximately 200°C. the blue solid was converted to a brown or black material which was shown in the First Quarterly Report[1] to be CuO. X-ray diffraction showed some loss of zeolite structure even in the Cu zeolites dried at < 150°C.

1.2 X-RAY DIFFRACTION STUDIES

Samples of NaA, LiA, KA, AgA, CaA_2, NaX, LiX, AgX, CaX_2, NaY and LiY were prepared and submitted for X-ray diffraction studies. X-ray diffraction patterns were used in this study to determine if the various methods of preparation of Type Y zeolites were successful and to determine if the zeolite crystal structure was preserved with cation exchange and activation. In addition the effect of the cation upon the spacing of the crystal planes was determined.

Powder diffraction patterns were taken on a Norelco Phillip Spectrometer using filtered Cu-K_α radiation. The results for the three types of zeolite containing various cations are given in Tables I, II, and III. The Miller indices (h, k, l) were assigned from the relation

$$m = h^2 + k^2 + l^2$$

where m was determined by the slide rule method from the d-spacings (2). Using this method it was found that the Type A zeolit s had a simple cubic structure with a unit cell length of approximately 12.3 A; Type X zeolite had a face centered cubic structure with a unit cell length of 25.0 A; and Type Y, face centered cubic with 24.7 A. Values of d-spacings as reported in the literature are given for comparison. The spacings for the Type A material are taken from reference (3), for the Type X from reference (4), and for the type Y from reference (5). All materials, with the exception of CuA_2, were vacuum activated at 350°C. before determining the diffraction patterns. CuA_2 was temperature sensitive and therefore was activated at 150°C. The peaks for the CuX_2 zeolite were present on the top of a high background level indicating some structure degradation of the zeolite had occurred.

The diffraction patterns show that the synthetic crystalline zeolites can be prepared in various cation forms, with the exception of Cu^{+2}, by ion exchange without altering the crystal structure to any great extent.

TABLE I

X-RAY DIFFRACTION DATA -d SPACINGS FOR TYPE A ZEOLITES

d, Å

m	h,k,l	NaA		LiA	KA	AgA	CaA_2		CuA_2
		Lit.	Obs	Obs	Obs	Obs	Lit.	Obs	Obs
1	100	12.294	12.39	12.18	12.30	12.30	12.243	12.35	12.27
2	110	8.706	8.70	8.53	8.70	8.75	8.664	8.70	8.66
3	111	7.109	7.12	6.96	7.13	7.08	7.075	7.10	6.96
4	200	-	-	-	6.19	6.15	6.121	6.16	6.17
5	210	5.508	5.50	5.39	5.50	5.50	5.478	5.50	5.47
6	211	5.031	5.03	-	5.12	-	5.002	-	5.01
8	220	4.357	4.35	4.27	-	4.33	-	-	4.33
9	221,300	4.107	4.09	4.01	4.09	4.08	4.084	4.09	4.07
10	310	-	3.86	3.80	3.90	3.87	3.875	-	3.88
11	311	3.714	3.69	3.63	3.70	3.69	3.696	3.70	3.69
12	222	-	-	-	3.55	3.545	3.539	-	3.56
13	320	3.417	3.40	3.34	3.40	3.411	3.398	3.40	3.40
14	321	3.293	3.28	3.21	3.29	3.300	3.276	3.28	3.27
16	400	-	-	-	3.08	-	-	3.18	3.05
17	410,322	2.987	2.98	2.92	2.98	3.076	2.972	2.99	2.966
18	411,330	2.904	2.89	2.84	2.90	2.976	2.888	2.90	2.880
19	331	-	-	-	-	2.891	-	-	2.810
20	420	2.754	2.74	2.69	2.75	2.740	2.741	2.74	2.740
21	421	2.688	2.69	2.63	2.69	2.680	2.676	-	2.665
22	332	2.626	2.62	2.57	2.62	2.619	2.614	2.62	2.608

TABLE II

X-RAY DIFFRACTION DATA - d SPACINGS FOR TYPE Y ZEOLITE

		d, °A								
		NaX		LiX		AgX		CaX_2		CuX_2
M	h,k,l	Lit	Obs	Lit	Obs	Lit	Obs	Lit	Obs	Obs
3	111	14.47	14.48	14.37	14.25	14.37	14.60	14.37	14.48	14.24
8	220	8.85	8.84	8.79	8.75	8.82	8.84	8.79	8.84	8.58
11	311	7.54	7.54	7.49	7.49	7.54	7,56	7.51	7.56	-
12	222	-	-	-	-	-	-	-	-	6.92
16	400	-	-	-	-	6.23	6.25	-	-	-
19	331	5.73	5.73	5.70	5.68	-	-	5.71	5.71	5.60
27	333,511	4.81	4.81	4.79	4.77	4.80	4.79	4.79	4.79	4.70
32	440	4.42	4.41	4.40	4.37	4.41	4.40	4.40	4.39	-
35	531	4.23	4.22	4.21	-	4.22	4.21	-	-	-
36	600	-	-	-	-	-	-	-	-	4.07
40	620	3.946	3.93	3.931	3.91	-	-	3.936	3.92	-
43	533	3.808	3.80	3.794	3.76	3.805	3.79	3.800	3.79	-
44	622	3.765	-	3.749	-	3.760	3.75	3.754	-	-
48	444	3.609	-	3.590	3.56	3.603	3.587	3.593	3.58	-
51	551,711	3.500	-	3.482	3.46	3.494	3.490	3.486	3.48	3.46

TABLE II

(Continued)

		d, ^{c}A								
		NaX		LiX		AgX		CaX_2		CuX_2
M	h,k,l	Lit	Obs	Lit	Obs	Lit	Obs	Lit	Obs	Obs
56	642	3.338	3.33	3.324	3.30	3.335	3.324	3.328	3.31	3.28
59	553,731	3.253	3.25	3.239	3.21	3.250	3.241	3.241	3.22	-
67	733	3.051	3.04	3.040	3.02	-	-	3.041	3.025	-
68	-	-	-	-	-	3.027	3.02	-	-	-
72	660,822	2.944	2.94	2.933	2.92	2.941	2.928	2.934	2.919	-
75	555,751	2.885	2.88	2.874	2.86	2.882	2.865	2.875	2.864	-
76	-	-	-	-	-	-	-	-	-	-
80	840	2.794	2.79	2.782	2.76	2.792	2.778	2.783	2.764	-
83	753,911	2.743	2.74	2.730	2.70	2.739	2.720	2.732	2.720	-
88	664	2.663	2.66	2.653	2.63	2.662	2.650	2.653	2.642	-
91	931	2.620	2.61	2.609	-	2.617	2.605	2.610	2.597	-
96	-	2.550	2.55	2.542	-	2.549	2.538	-	-	-

TABLE III

X-RAY DIFFRACTION DATA -d SPACINGS FOR TYPE Y ZEOLITES

m	hkl	d, Å NaY Lit.	d, Å NaY Obs.	d, Å LiY Obs.
3	111	14.3	14.4	14.36
8	220	8.73-.80	8.75	8.84
11	311	7.45-.50	7.46	7.53
12	222	-	-	-
16	400	-	-	-
19	331	5.67-.71	5.68	5.68
27	333, 511	4.75-.79	4.74	4.76
32	440	4.37-.46	4.36	4.37
35	531	-	-	-
36	600	-	-	-
40	620	3.90-.93	3.90	3.90
43	533	3.77-.79	3.76	3.76
44	622	-	-	-
48	444	3.57-.59	3.56	3.56
51	551, 711	3.46-.48	3.45	3.45
56	642	3.30-.33	3.30	3.30
59	553, 731	3.22-.24	3.21	3.21
67	733	3.02-.04	3.02	3.01
68	-	-	-	-
72	660, 822	2.90-.93	2.91	2.91
75	555, 751	2.85-.87	2.85	2.85
76	-	-	-	-
80	840	2.76-.78	2.74	2.76
83	753, 911	2.71-.73	2.71	2.70
88	664	2.63-.65	2.63	2.63
91	931	2.59-.61	2.59	2.58
96	844	2.52-.54	2 53	-

1.3 DETERMINATION OF IONIC CONDUCTIVITY

The ionic conductivity of selected zeolites can be determined from a measurement of the resistance as a function of temperature. Zeolite pellets with integral gold foil electrodes were prepared by vacuum hot pressing. The pellets formed by this technique are 0.5 inches in diameter with a thickness in the range of 0.040-0.050 inches. Prior to conductivity measurements, the zeolite pellets are activated and adsorbed water removed by heating to 400°C for 16 hours at low pressures. The resistance of the pellet was measured with an Electro-Measurements Inc. Impedance Bridge, Model 250 DA using a Hewlett-Packard AC voltmeter, Model 400 D as the detector. Other details of sample preparation and measurement are given in the First Quarterly Report (1).

1.3.1 RESISTANCE MEASUREMENTS

The resistance as a function of temperature has been determined for NaX, AgX, LiX, NaY, LiY, and NaA zeolites. In addition a study of the effect of various binders and binding treatments on the resistances was initiated.

The effect of the cation on the resistance of Type X zeolites is shown in Table IV and Figure 1. At the time the measurements were made, AgX was of interest as a cathode depolarzer in a solid state battery. The higher resistance and greater coulombic attraction of the smaller Li^+ is readily apparent.

Tables V and VI and Figures 2 and 3 show the effect of zeolite type upon resistivities. The Y zeolites were synthesized in our laboratories by the procedure given in Section 1.1.1 The activation energy for conduction for NaY was found to be 15.0 kilocalories per mole. Calculations using the activation energy yield the following composition of the unit cell after dehydration

$$Na_{63} \quad \left[(AlO_2)_{63} \quad (SiO_2)_{129}\right]$$

The activation energy for LiY was 20 kilocalories per mole which is higher than the 15 kcal/mole found for NaY. This higher energy requirement is another manifestation of the stronger attachment of lithium ions in the zeolite lattice.

Both phosphoric acid and sodium silicate are being considered as sintering aids for the fabrication of thin zeolite membranes (see Section 1.4). The effect of these sintering aids upon the resistivity of NaA zeolite was investigated. For these investigations dry powders of either the pure NaA zeolite or NaA zeolite containing the desired sintering aid were fabricated into thin membranes having integral gold foil electrodes by the vacuum hot pressing technique as reported before. The results for the NaA and NaA containing phosphoric acid and sodium silicate are shown in Table VII and Figure 4.

TABLE IV

EFFECT OF CATIONS ON THE RESISTIVITY OF TYPE X ZEOLITES

NaX		LiX		AgX	
Temperature °C	Resistivity ohm-cm	Temperature °C	Resistivity ohm-cm	Temperature °C	Resistivity ohm-cm
155	9.55×10^4				
210	1.61×10^4	225	2.8×10^4	225	1.9×10^3
265	3.44×10^3	315	5.5×10^3	315	1.2×10^3
300	1.89×10^3	385	1.4×10^3	385	7.7×10^2
335	1.11×10^3	450	6.2×10^2	460	5.7×10^2
400	4.04×10^2	485	4.8×10^2		
470	2.66×10^2				
510	2.33×10^2				
535	1.77×10^2				

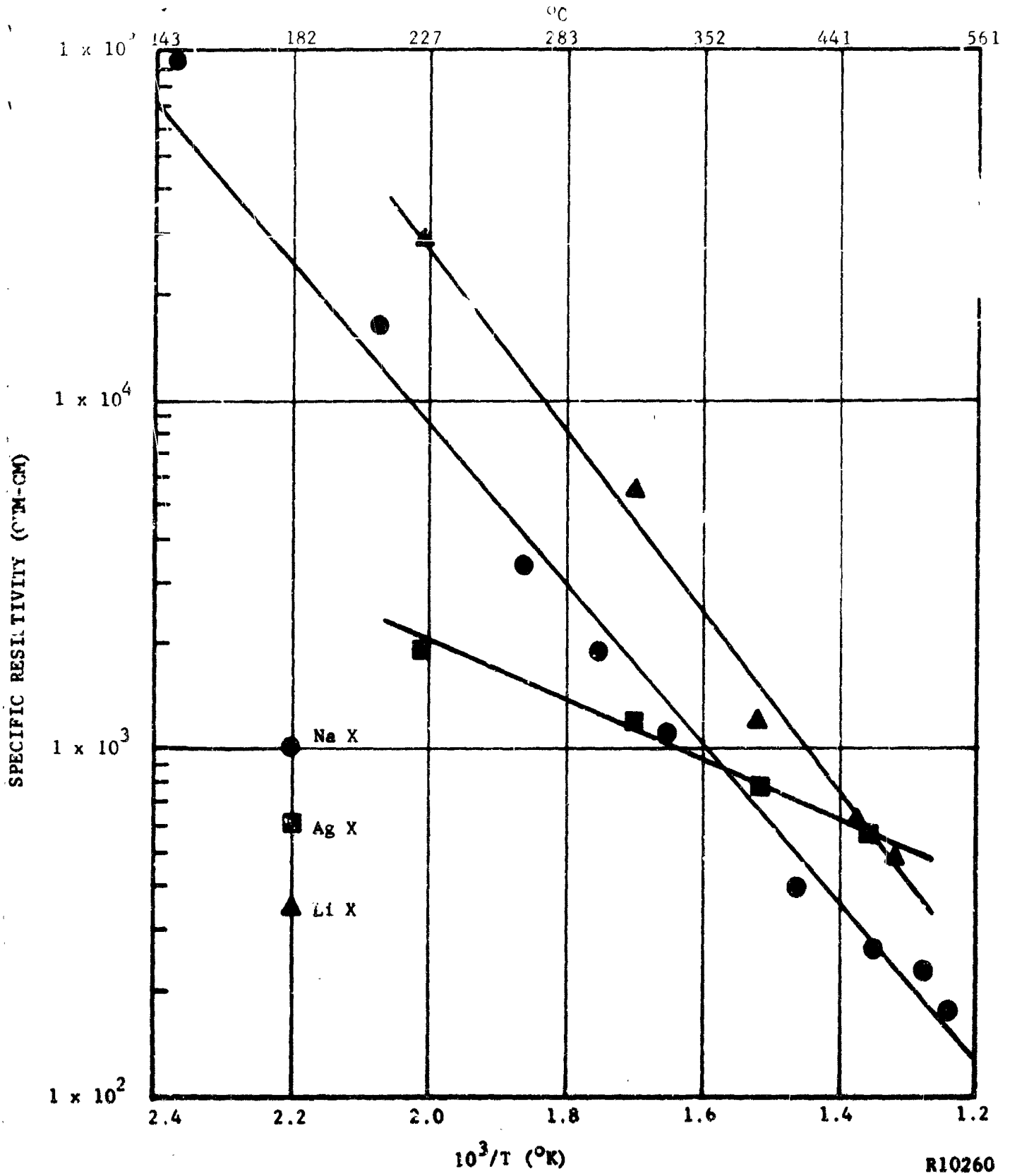

FIGURE 1. EFFECT OF CATION ON RESISTIVITY OF TYPE X ZEOLITE

TABLE V

EFFECT OF ZEOLITE TYPE ON RESISTIVITIES OF SODIUM ZEOLITES

NaA		NaY		NaX	
Temperature °C	Resistivity ohm-cm	Temperature °C	Resistivity ohm-cm	Temperature °C	Resistivity ohm-cm
25	3.5×10^7	200	1.3×10^6	155	9.55×10^4
135	2.6×10^6	270	1.4×10^5	210	1.61×10^4
165	1.6×10^6	315	4.5×10^4	265	3.44×10^3
185	3.8×10^5	395	9.1×10^3	300	1.89×10^3
215	2.94×10^5	445	4.2×10^3	335	1.11×10^3
245	1.7×10^5	480	2.7×10^3	410	4.04×10^2
280	6.4×10^4			470	2.66×10^2
315	3.1×10^4			510	2.33×10^2
360	1.7×10^4			535	1.77×10^2
390	1.0×10^4				
440	6.1×10^3				
475	3.4×10^3				

TABLE VI

EFFECT OF ZEOLITE TYPE ON RESISTIVITIES OF LITHIUM ZEOLITES

LiX		LiY	
Temperature °C	Resistivity ohm-cm	Temperature °C	Resistivity ohm-cm
225	2.8×10^4	205	6.6×10^7
315	5.5×10^3	270	4.5×10^5
385	1.4×10^3	330	7.0×10^4
450	6.2×10^2	390	1.6×10^4
485	4.8×10^2	450	5.6×10^3
		495	3.3×10^3

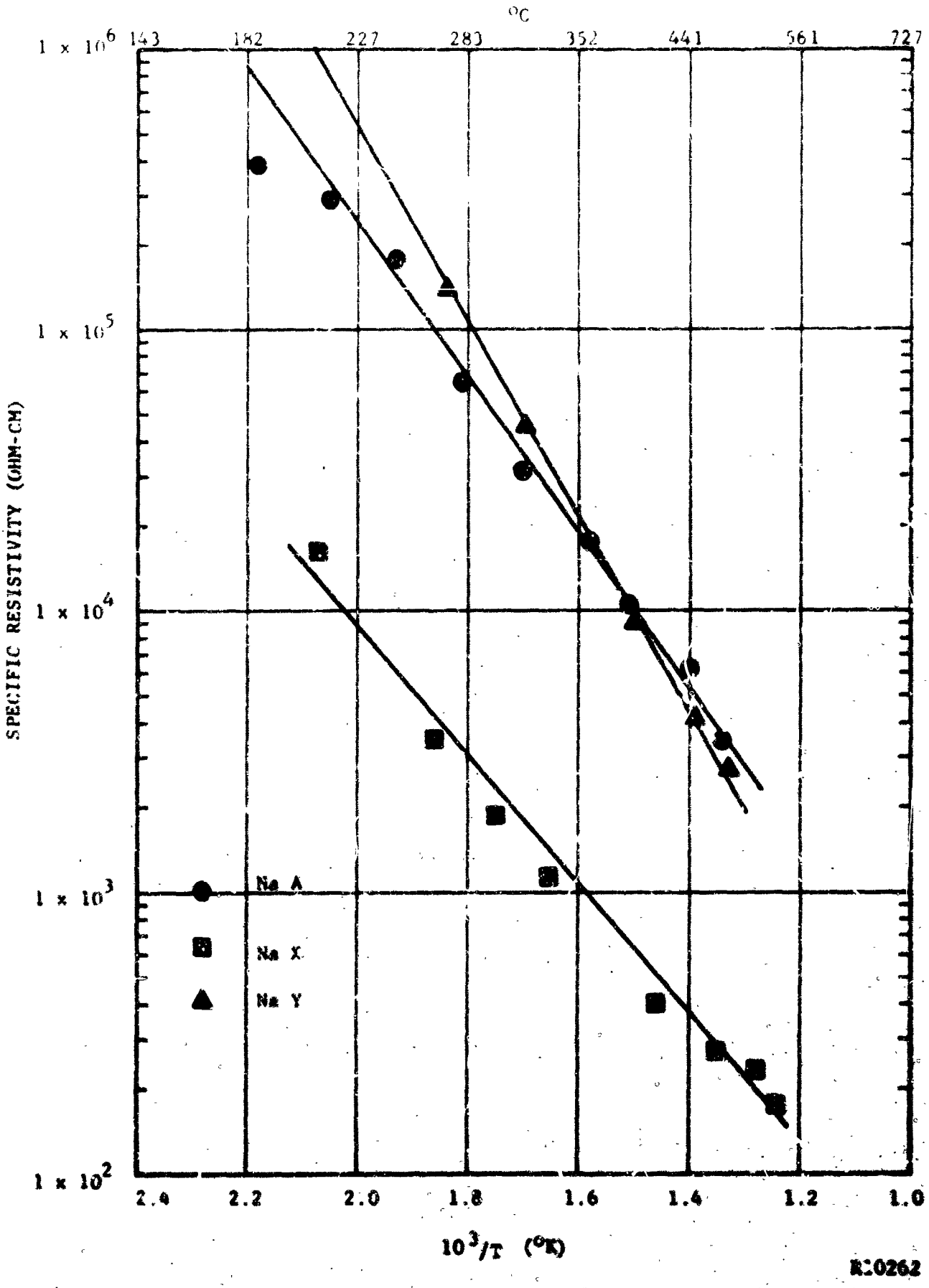

FIGURE 2. EFFECT OF ZEOLITE TYPE ON RESISTIVITIES OF SODIUM ZEOLITES

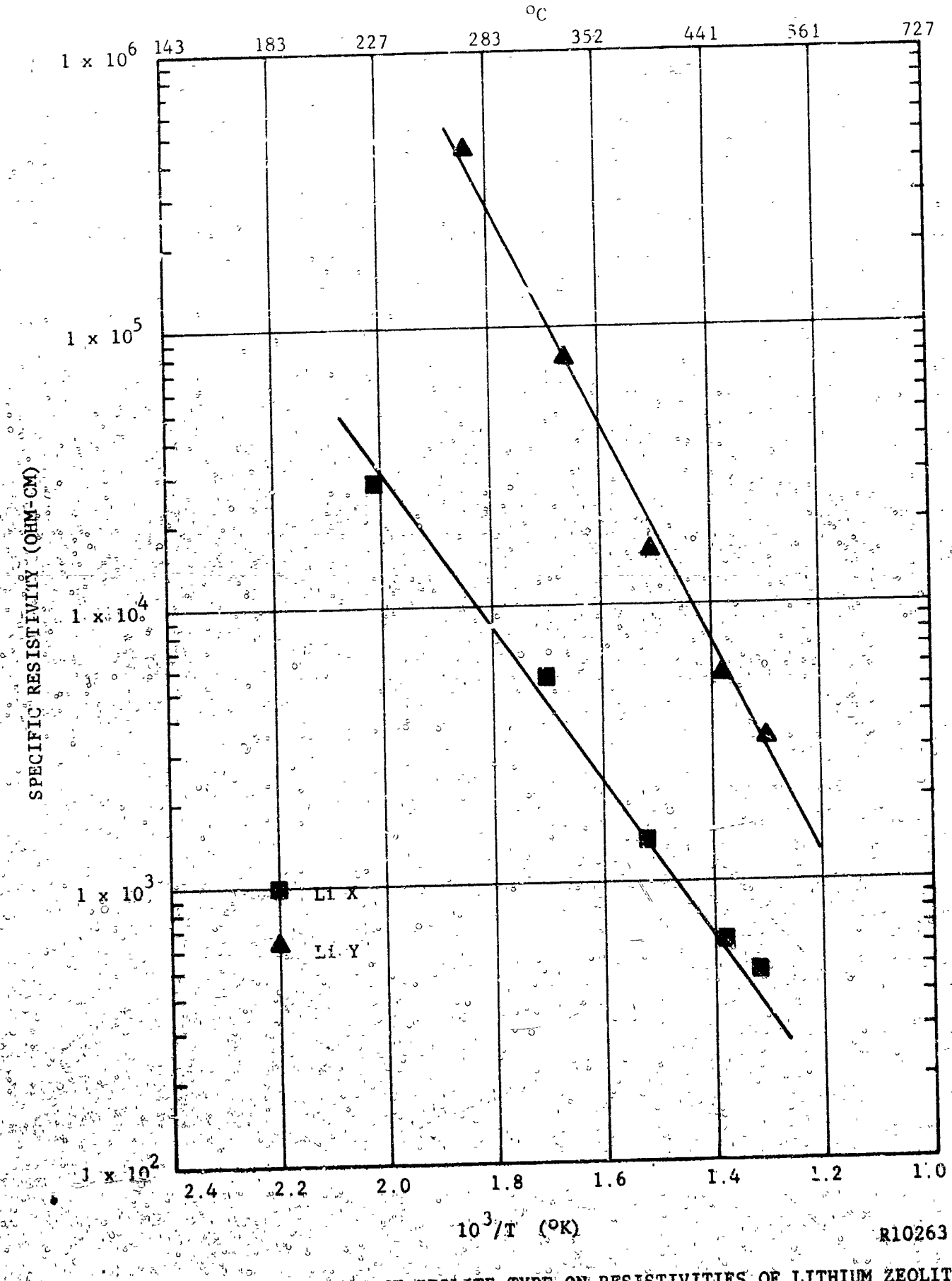

FIGURE 3. EFFECT OF ZEOLITE TYPE ON RESISTIVITIES OF LITHIUM ZEOLITES

TABLE VII

EFFECT OF H_3PO_4 AND $Na_2Si_2O_5$ ON RESISTIVITY OF NaA ZEOLITE

NaA (Pure)		$NaA(H_3PO_4)$, Z-5		$NaA(Na_2Si_2O_5)$, Z-3	
Temperature °C	Resistivity ohm-cm	Temperature °C	Resistivity ohm-cm	Temperature °C	Resistivity ohm-cm
135	2.6×10^6	90	3.8×10^7		
165	1.6×10^6	210	9.4×10^6	210	3.0×10^6
185	3.8×10^5	285	1.9×10^6	260	3.7×10^5
215	2.9×10^5	330	7.6×10^5	315	8.5×10^4
245	1.7×10^5	350	4.6×10^5	325	7.8×10^4
280	6.4×10^4	380	2.8×10^5	380	2.1×10^4
315	3.1×10^4			395	2.7×10^4
360	1.7×10^4	445	9.4×10^4	450	1.0×10
390	1.0×10^4	475	5.3×10^4	460	7.8×10^3
440	6.1×10^3	485	4.3×10^4	505	4.9×10^3
475	3.4×10^3			530	3.7×10^3

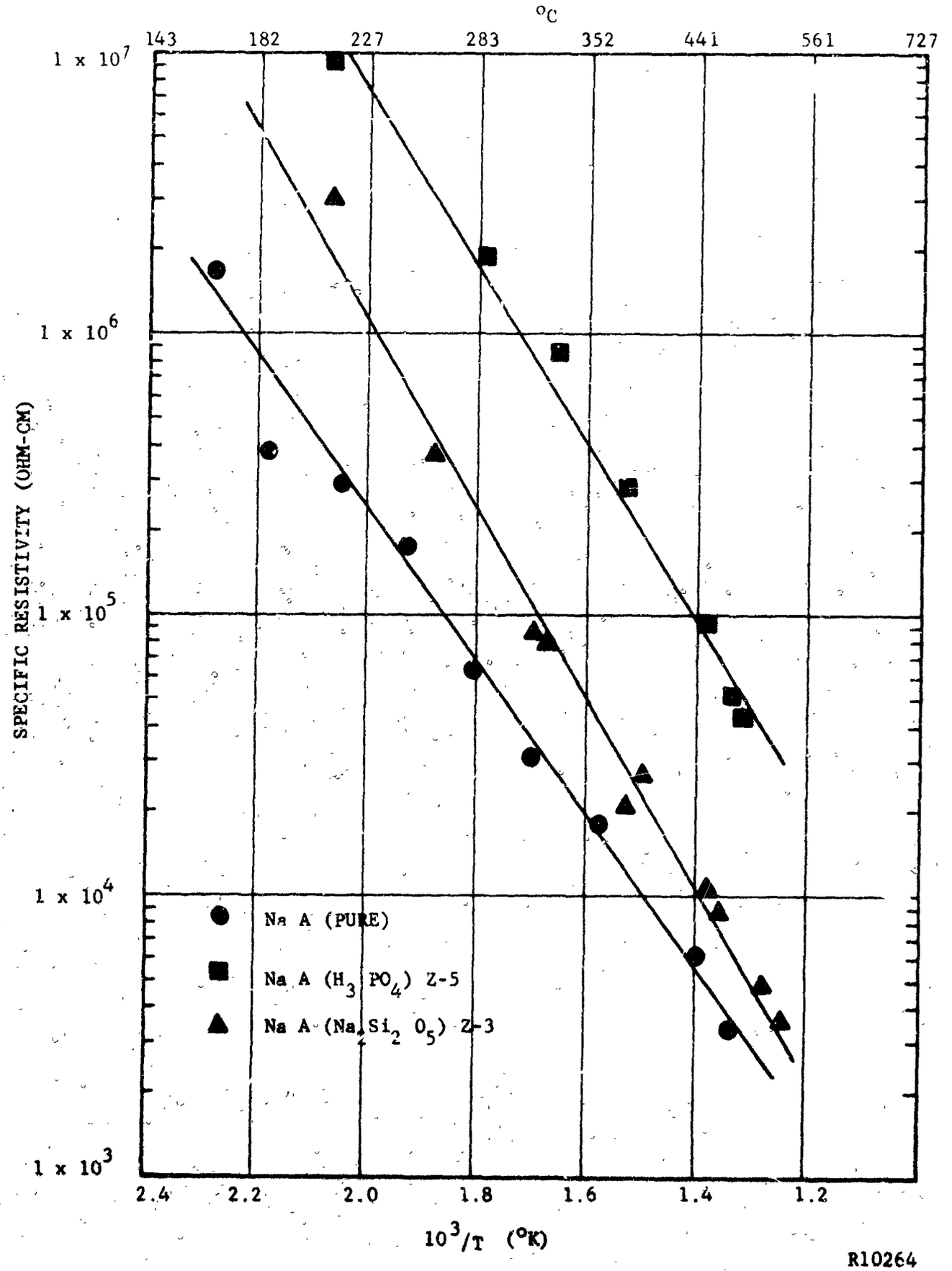

FIGURE 4. EFFECT OF H_3PO_4 AND $Na_2Si_2O_5$ BINDERS ON RESISTIVITY OF NaA ZEOLITES

The silicate sample (Z-3) contained 20 weight percent of $Na_2O \cdot 2SiO_2$ and the phosphoric acid sample (Z-5) contained 18% phosphoric acid and 2% of an aqueous solution of polyvinyl alcohol. As the experimental results indicate, the addition of either phosphoric acid or sodium silicate caused an increase in the resistance of vacuum hot pressed NaA membranes. This effect of silicate is much smaller than that of phosphoric acid. A much greater increase in resistivity is noted with the H_3PO_4 treated material. It appears that the H_3PO_4 interacts with the zeolite alumino-silicate lattice in such a way as to reduce either the number of charge carriers or their mobility. This effect has also been noted with other acids.

Zeolite membranes prepared by sintering at higher temperatures using H_3PO_4 or sodium silicate as a binder had a smooth, hard surface. No suitable method of attaching gold leaf electrodes for conductivity measurements could be found for these membranes. Therefore, two other methods of attaching metallic electrodes were tried. In the first methods, a silver electrode was formed on the surface of the fired zeolite membrane by covering with a silver conducting paste. Samples prepared in this manner had a resistance of about 10^6 ohms at 65°C and showed practically no variation of resistance with temperature, thereby indicating that adequate contact was not achieved between the zeolite membrane and the silver electrode.

Considerably better results were obtained with gold electrodes placed on the surface of the membrane by vacuum evaporation. Table VIII gives the resistivity of a hot pressed NaA membrane with vacuum evaporated gold electrodes. Figure 5 compares the resistivity of hot pressed NaA membranes with gold leaf and with evaporated gold electrodes. The results indicate practically no difference in the two techniques. Thus vacuum evaporation of gold appears to be a suitable method of attaching electrodes to formed zeolite wafers.

The effect of heat treatment at 740°C and phosphoric acid upon the resistance of NaX is shown in Table IX and Figure 6. These results are based on only preliminary investigations in bonding NaX zeolites. It is expected that further experimentation will produce bonded zeolite membranes with lower resistances. The hot pressed membranes were made in the usual manner. The phosphate bonded zeolite (Z-14, 27 weight % H_3PO_4) had been heated to 740°C. Evaporated gold foil electrodes were used. From the results it appears that the NaX can be heated to approximately 700°C with no change in resistance unless phosphoric acid is present. At the time this report was written, no samples of NaX bonded with silicate were available.

A thin (0.0485 in.) zeolite membrane was obtained from Astropower Laboratory of Douglas Aircraft Co., Inc. for possible use in this application. This membrane was made from Zeolon H, H_3PO_4 and ZrO_2 and had their designation Lot No. 851-21. The resistance of this membrane was measured as a function of temperature while under vacuum. The results are given in Table X. The relatively constant values of resistivity in the temperature range 160° to 450°C could indicate destruction of the zeolite lattice structure at higher

TABLE VIII

RESISTIVITY OF HOT PRESSED NaA ZEOLITE WITH EVAPORATED GOLD ELECTRODES

Gold Foil		Evaporated Gold	
Temperature °C	Resistivity ohm-cm	Temperature °C	Resistivity ohm-cm
135	2.6×10^6	25	1.5×10^7
165	1.6×10^6	55	7.4×10^6
185	3.8×10^5	175	5.9×10^5
215	2.9×10^5	235	8.2×10^4
245	1.7×10^5	290	3.9×10^4
280	6.4×10^4	335	2.3×10^4
315	3.1×10^4	395	1.5×10^4
360	1.7×10^4	450	5.4×10^3
390	1.0×10^4	505	2.8×10^3
440	6.1×10^3		
475	3.4×10^3		

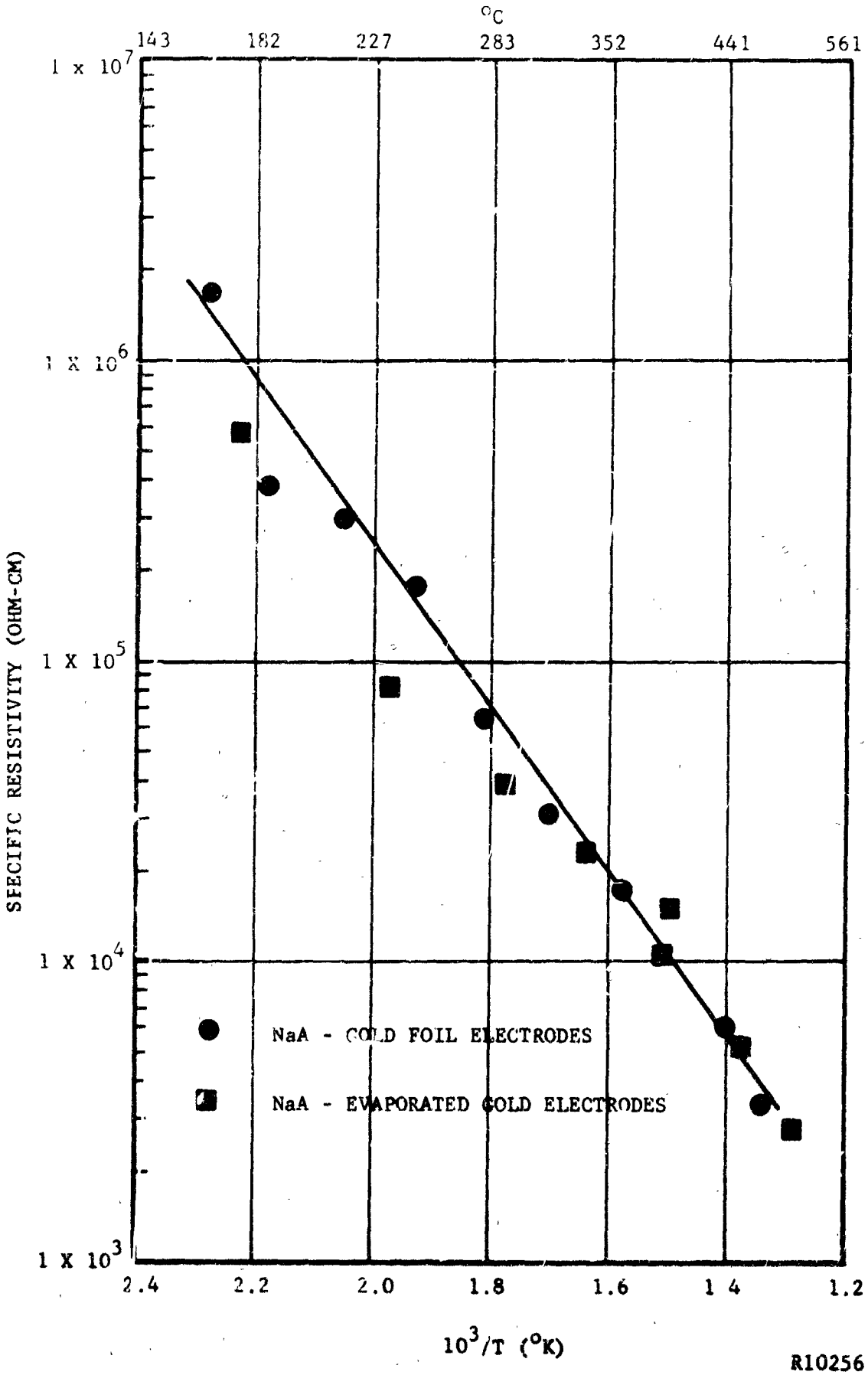

FIGURE 5. COMPARISON OF GOLD FOIL AND EVAPORATED GOLD ELECTRODES. NaA ZEOLITE-HOT PRESSED

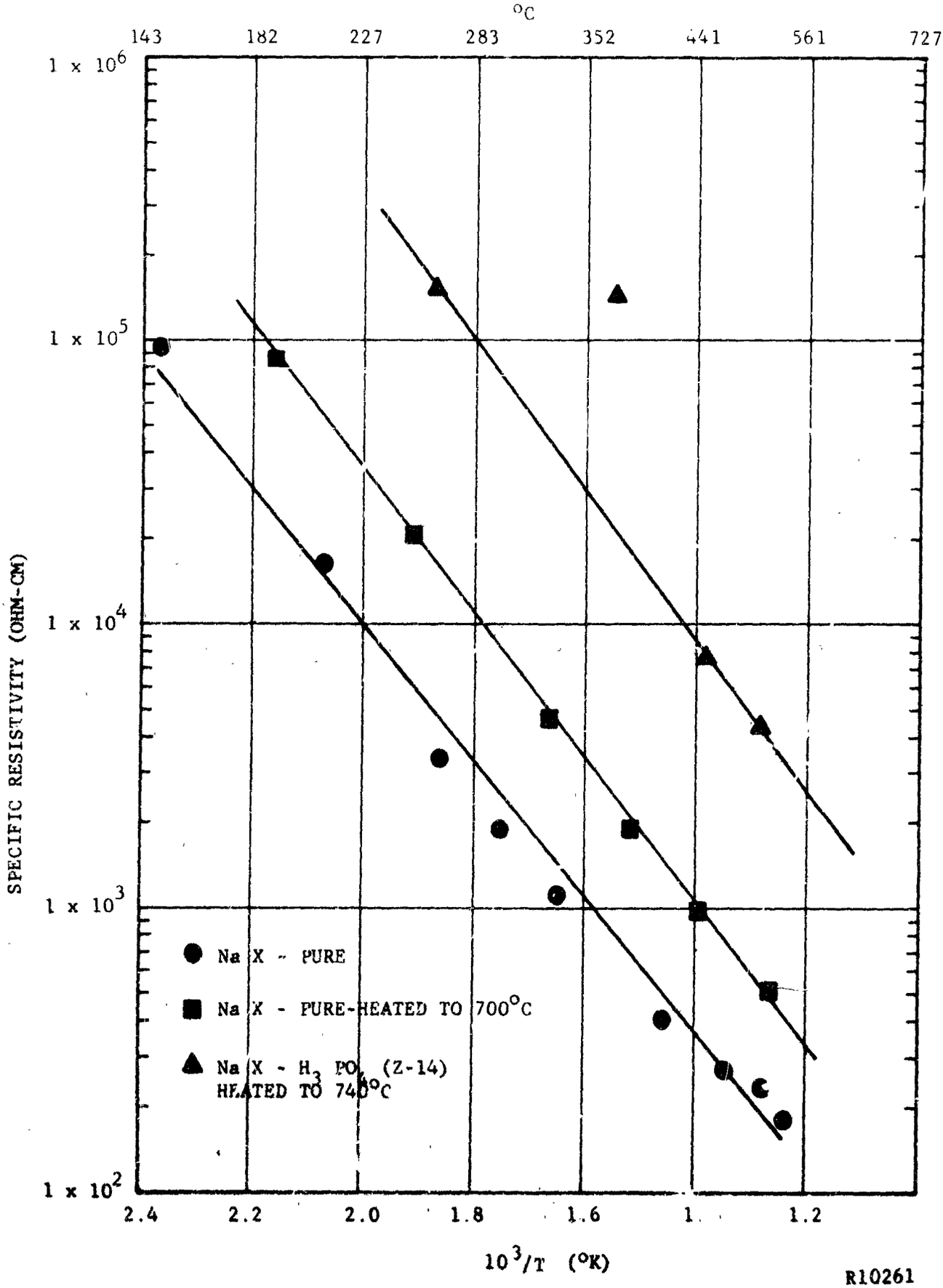

FIGURE 6. EFFECT OF HEAT TREATMENT AND H_3PO_4 ON THE RESISTIVITY OF NaX ZEOLITE

TABLE IX

EFFECT OF HEAT TREATMENT AND H_3PO_4 ON THE RESISTIVITY OF NaX ZEOLITES

NaX-Pure Hot Pressed		NaX-Pure Hot Pressed Heat Treated @ 700°C		NaX-H_3PO_4 (%-14) Heat Treated @ 740°C	
Temperature °C	Resistivity ohm-cm	Temperature °C	Resistivity ohm-cm	Temperature °C	Resistivity ohm-cm
155	9.6×10^4	120	4.4×10^5	195	1.2×10^7
210	1.6×10^4	190	8.4×10^4	260	1.6×10^5
265	3.4×10^3	250	2.1×10^4	382	1.4×10^5
300	1.9×10^3	325	4.7×10^3	445	7.6×10^3
335	1.1×10^3	385	1.9×10^3	505	4.2×10^3
410	4.0×10^2	440	1.0×10^3		
470	2.7×10^2	515	5.2×10^2		
510	2.3×10^2				
535	1.8×10^2				

TABLE X

RESISTIVITY OF ASTROPOWER ZEOLON

MEMBRANE LOT NO. 851-21

Temperature °C	Resistivity ohm-cm
25	3×10^7
85	2×10^7
110	1×10^7
160	6.9×10^6
210	3.5×10^6
255	5.5×10^6
305	5.0×10^6
350	8.0×10^6
430	4.0×10^6

temperature by fixation of hydrogen ions in the alumino-silicate framework [illegible]m OH groups with the resulting elimination of hydrogen ions as a conductive species. No further testing of these membranes is anticipated.

ZEOLITE BONDING AND SINTERING EXPERIMENTS

The goal of this phase of the programs was to develop a ceramic process suitable for the fabrication of thin 2 inch diameter zeolite A membranes. The ultimate thickness was to be on the order of 10-15 mils. Dry pressing and sintering was considered the most appropriate process for investigation.

The main problem in the sintering approach was the relatively low transformation temperature (700°-800°C) reported for the zeolite structure. The second problem concerned the effect of a sintering aid on the zeolite structure and its exchange properties. Three materials were considered as sintering aids; they were: sodium silicate, phosphoric acid, and sodium metaphosphate. Sodium silicate was considered compatible (a raw material source for zeolite synthesis) with sodium Zeolite A. It also has an eutectic melting point of 780°C, with a sintering range of 700-800°C. Phosphoric acid was selected for its cementing reaction which the alumino-silicate materials and possible formation of phosphate glass bonds. Sodium metaphosphate, an anhydrous phosphate glass with a melting point of 630°C, was selected for its glass forming properties. An additional consideration for the selection of phosphate materials was attributed to the speculation that phosphate glasses may exhibit resistance to liquid sodium corrosion, the anode being investigated in this project.

1.4.1 EXPERIMENTAL PROCEDURE

The zeolite A power was first saturated with distilled water followed by the appropriate addition of sodium silicate or phosphoric acid. The material was then granulated by hand in a glass drying dish as it was intermittently dried in an oven (80°C) or over a hot plate. The bonding of the material during granulation formed particles that were readily separated into a minus 80 plus 200 mesh fraction for dry pression. Additions of an organic binder (polyvinyl alcohol, PNA) to promote granulation resulted in poor sintered strength and was abandoned. Following final drying at 80°C, the powder was pressed in a 1/2 inch diameter Meehenite die with heat treated drill rod punches. No lubricant or anti-sticking additions were required. Sintering times and temperatures were initially based on DTA (differential thermal analysis) and TGA (thermogravimetric analysis) of the raw zeolite and sintering compositions. X-ray analysis was the final criteria for verifying the structure of the sintered zeolite. Sintering was performed in a tube furnace operated between 700°C and 800°C. The samples were preheated on a refractory slab in the entrance of the tube to approximately 300°C for 10 minutes and then pushed into the firing zone for a specified time. The samples were withdrawn from the hot zone and cooled in the entrance for 5 minutes before removing to room temperature. The fired discs were inspected for

scratch hardness and shrinkage. Those samples exhibiting good strength were then submitted for X-ray diffraction. Optimum times, temperature, and compositions relationships were established crystallographically by this means to ensure the maintenance of the zeolite A structure. Additional sintering experiments were conducted on the most promising compositions to increase their fired densities, the objective being to reduce the intergranular pore volume to a closed pore condition, thus leaving the molecular pore of the zeolite as the principal connecting pore system. Density measurements were made by the volume displacement method in water on saturated specimens. This technique allowed comparison to published data (3) utilizing the same procedure.

1.4.2 RESULTS

Initial DTA data indicated that zeolite A began a transformation at 770°C. In the presence of phosphoric acid the first perceptible transformation occurred at 850°C. TGA data showed dehydration and activation was complete at 400°C. Both analysis were run at a temperature rise of 10°C/minute.

Table XI shows the compositions containing phosphoric acid and sodium silicate investigated during this period. Samples Z-2, 3, and 4 were initial exploratory compositions made for sintering observations and X-ray analysis. Table XII, X-ray diffraction data, confirmed the DTA information in showing that the sodium silicate materials, Z-3, readily transformed at 810°C, while the phosphoric acid materials, Z-5, retained their structure at 800°C. Table XII also shows the complete disintegration of the raw zeolite, NaA, when heated to 880°C. This material was taken from a DTA run. The first column headed NaA contains the diffraction data obtained on the powder as received. Table XII is representative of the data obtained; the intensities, though not indicated, varied with hydration as described in the literature (3).

Following the preliminary evaluations of Z-2, 3, and 4, two series of compositions were prepared to determine the effects of concentration on strength, crystal structure, and sinterability. Z-7, 8, and 10 yielded good structures and strength in 15 mil, 1/2 inch diameter discs that survived 3 feet drop test. Sintering at 740°C for 30 minutes resulted in little detectable distortion of the zeolite lattice parameters for compositions containing either 10% phosphoric acid or 21% sodium silicate;Z-8 containing 10% phosphoric acid appeared to be stronger than Z-10 containing 21% sodium silicate.

Sintering results shown in Table XIII indicate the relative shrinkage and scratch resistance of the compositions sintered at 700, 740, and 780°C for 30 minutes, respectively. Z-8 appears to contain about the minimum amount of phosphoric acid for acceptable sintering. Z-10 and Z-11 were both well sintered at 780°C, however, Z-10 at 740°C is favored due to the on-set of transformation in the sodium silicate compositions above 770°C.

TABLE XI

SINTERING COMPOSITIONS FOR TYPE A ZEOLITES

No.	Wt. % Zeolite	Wt. % Binder	Binder
Z-2	90	10	H_3PO_4
Z-3	80	20	$Na_2O \cdot 2SiO_2$
Z-4	70	30	H_3PO_4
Z-5	80	18 + 2 PVA	H_3PO_4
Z-6	69	31	H_3PO_4
Z-7	82	18	H_3PO_4
Z-8	90	10	H_3PO_4
Z-9	95	5	H_3PO_4
Z-10	79	21	$Na_2O \cdot 2SiO_2$
Z-11	89	11	$Na_2O \cdot 2SiO_2$
Z-12	94	6	$Na_2O \cdot 2SiO_2$
Z-13	96.5	3.5	$Na_2O \cdot 2SiO_2$
Z-N	80	18 + 2 PVA	$NaPO_3$

Materials added as:

Phosphoric Acid - 85% H_3PO_4

Sodium Silicate - N Brand - 1% $Na_2O \cdot 2SiO_2$

PVA - Polyvinyl Alcohol - 2% Aqueous Solution

TABLE XII

TYPICAL X-RAY DIFFRACTION DATA OF SINTERED TYPE A ZEOLITES

h,k,l	NaA	NaA (880°/10°C/min)	Z-3 (810°/10min)	Z-5 (800°/10min)	Z-7 700°/30min	Z-8 740°/30min	Z-10 740°/30min	Z-N 750°/30min
100	12.23	-	11.93	12.44	12.35	12.26	12.26	12.09
110	8.66	-	8.49	8.75	8.70	8.65	8.66	8.63
111	7.04	-	6.96	7.13	7.09	7.04	7.07	7.02
210	5.48	-	5.39	5.51	5.48	5.48	5.48	5.45
211	4.99	-	-	5.02	5.00	4.98	5.00	4.96
220	4.34	-	-	4.34	4.32	4.33	4.33	4.31
221	4.09	4.17	4.13 4.04	4.09	4.09	4.09	4.09	{4.26 4.07
311	3.79	3.60	3.67	3.70	3.70	3.70	3.70	3.69
320	3.40	3.31	3.37	3.41	3.41	3.40	3.40	3.39
321	3.28	3.26	3.25	3.28	3.28	3.27	3.28	3.27
410	2.99	3.02	2.99	2.98	2.98	2.97	2.98	2.97
411	2.89	-	2.96	2.89	2.90	2.90	2.89	2.89
420	2.76	-	-	2.75	2.75	2.74	2.74	2.74
421	2.68	-	-	2.68	2.68	2.68	2.68	2.67
332	2.62	2.55	2.59	2.61	2.61	2.61	2.61	2.61
422	2.49	2.49	2.54	2.50	2.51	2.50	2.50	2.49
430	2.45	-	-	2.45	2.45	2.45	2.45	2.45
511	2.37	2.35	-	2.35	2.35	2.35	2.36	2.35
520	2.28	-	-	-	-	-	-	-
521	2.24	-	-	-	2.24	2.24	-	2.24

TABLE XIII

SINTERING RESULTS TYPE A ZEOLITE

Composition	Sintered Diameter, Inches 700°C/30 Min.	740°C/30 Min.	780°C/30 Min.
Z-6	.458 h	.446 h	.430 h
Z-7	.475 h	.470 h	.460 h
Z-8	.487 s	.485 h	.480 h
Z-9	.494 c	.489 c	.489 c
Z-10	.494 s	.485 h	.444 w
Z-11	.496 c	.489 s	.451 h
Z-12	.498 c	.494 c	.475 s
Z-13	.500 c	.495 c	.473 c

w - warped
h - hard
s - soft
c - chalky

Table XIV shows the results of sintering experiments with the Z-7 composition to determine the relationship between mechanical pores due to consolidation and the molecular pores of the zeolite structure. Linde publishes a density of NaA of 1.99 gm/cm^3 (3). This was determined for a saturated structure, thus the column Sat. Density in Table XIV indicates the relative comparison. This measurement was made by the displacement technique in water following a weight determination after 4 hours of boiling in water. The % theoretical density column indicates little change from about 85% with sintering temperature. The % H_2O absorbed indicates a value of about 28%. Theoretical saturation has been reported to be 22.2%. The difference is assumed to represent the fabrication porosity between grains.

One exploratory experiment with sodium metaphosphate glass was conducted utilizing a 20% addition of $NaPO_3$, Z-N Table XI. The composition was ball milled for 4 hours with distilled water and granulated with a 2% PVA addition. In this case, as reported earlier, PVA appeared to be detrimental to good sintered strength. Future work should include minor additions of phosphoric acid for granulation purposes. X-ray data indicated a slight shift at high angles but good agreement at the low angle deflections. It may be concluded that sodium metaphosphate is also a suitable flux for binding Zeolite A structures.

1.4.3 CONCLUSIONS

Zeolite NaA was granulated, dry pressed, and sintered without destroying the zeolite structure by the addition of sintering aids of 10-20% phosphoric acid and 21% sodium silicate. Sintering temperature up to 800°C were utilized with phosphoric acid bonded zeolite NaA without excessive degradation of the crystal structure. Temperatures below 770°C were required to maintain the zeolite NaA structure with additions of sodium silicate. An 18% sodium metaphosphate addition also exhibited favorable sintering characteristic at 750°C. Zeolite NaA + 18% phosphoric acid sintered at 740°C for 45 minutes resulted in 86½% theoretical density and a water absorption of 28.7%. (Theoretical water absorption equals 22.2%). Samples 15 mil thick and 1/2 inch in diameter sintered at the above conditions readily sustained drop tests of 3 feet and resisted steel scratch indentation.

TABLE XIV

SINTERING-DENSITY RESULTS-COMPOSITION Z-7

Sinter °C/Min.	Dia. inch	Thick inch	Vol cm^3	Dry Wt gm	Sat Wt gm	Wt in H_2O gm	Calc Bulk Density gm/cm^3	Dry Density gm/cm^3	Sat Density gm/cm^3	% Theor Density	% H_2O Absorb
700/30	.476	.058	.169	.1987	.2755	.113	1.18	2.27	1.68	84	27.9
720/30	.474	.057	.164	.1955	.2715	.1106	1.19	2.30	1.69	85	28.0
740/45	.469	.057	.161	.1942	.2725	.1139	1.21	2.42	1.72	86.5	28.7
760/30	.468	.060	.169	.1976	.2791	.1161	1.17	2.42	1.71	86	29.2

SECTION 2

CATHODE STUDIES

The study of the electrochemical properties of selected cathode depolarizers has continued. These include cuprous chloride, cupric chloride, bismuth trichloride, ferric chloride, and silver chloride. These salts were also tested in the presence of diluents.

Electrode materials investigated include gold, tungsten, graphite, tantalum, boron carbide, and "Glassy Carbon".

Chronopotentiometric studies of short durations (up to several hours) were performed using the experimental cell described in the Section 2 of the First Quarterly Report (NASA CR-54208) and shown in Figure 8 of the same Report.

Longer term tests were carried out using the experimental arrangement described below.

ELECTROLYTIC CELL

A schematic diagram of the cell is shown in Figure 7. The cell container was a Pyrex tube 240 mm by 30 mm in outside diameter. Within the cell the cathode depolarizer was compartmented with a ceramic tube 170 mm long, 10.5 mm in outside diameter and 9 mm in inside diameter. The ceramic material was composed as follows:

SiO_2	54%
Al_2O_3	36%
Na_2O	9.6%
K_2O	0.4%

The ceramic was prepared as described by R. J. Labrie[7].

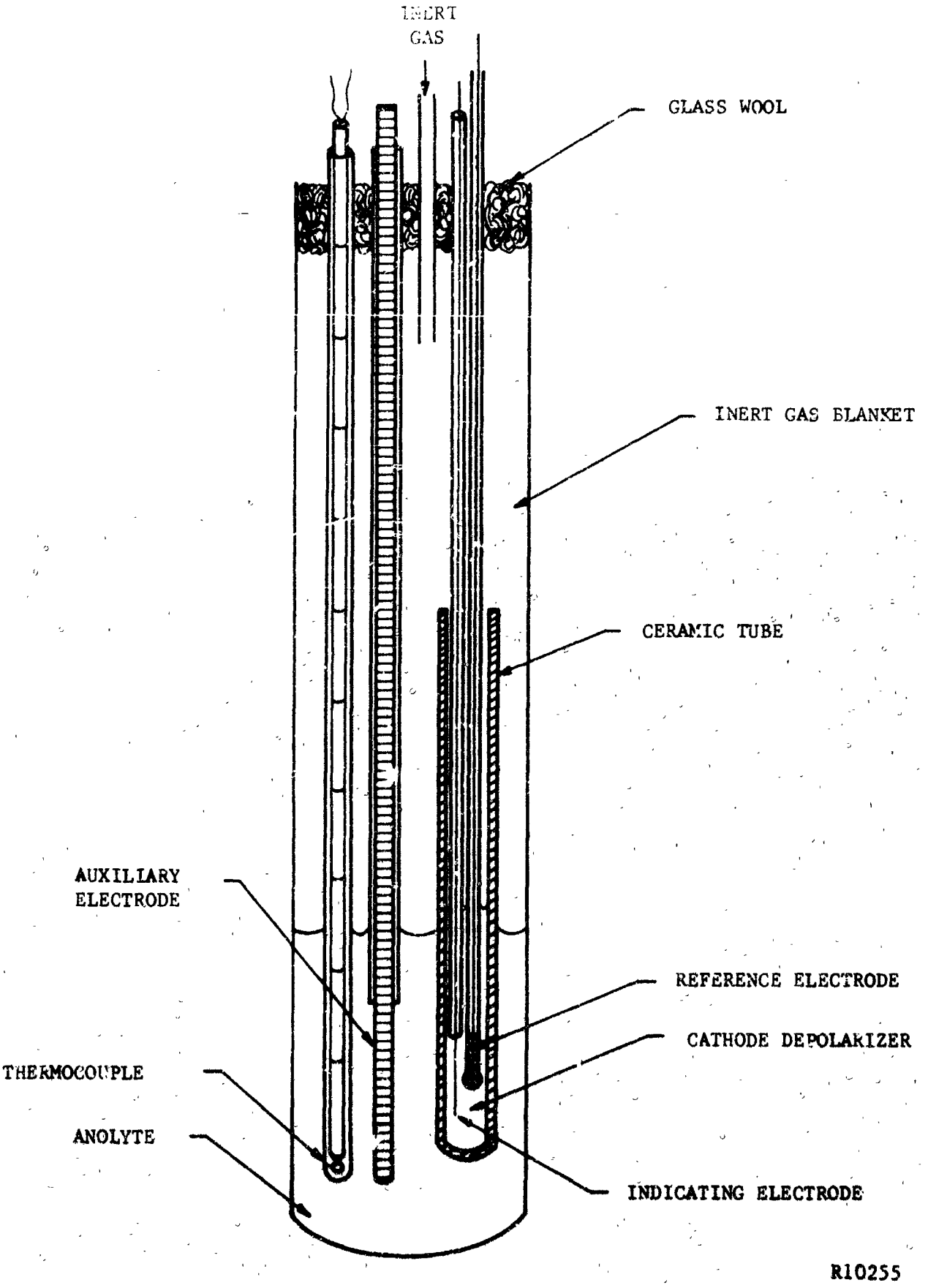

FIGURE 7. ELECTROLYSIS CELL

The indicator electrode was a wire of the material tested 25 mils in diameter projecting 16.7 mm from the closed lower end of a Pyrex tube 250 by 3.2 mm in diameter. The projected area of the electrode was 1/3 cm^2.

The auxiliary electrode was a spectrographically pure graphite rod 1/4 inch in diameter and one foot long projecting from the neds of a Pyrex sheath by about 2 cm. The density of the graphite was 1.9 g/cm^3.

The Ag - 0.13 m AgCl reference electrode was described in detail in the Section 2 of the First Quarterly Report (1).

The indicator electrode and the reference electrode were inserted in the ceramic tube containing the cathode depolarizer. The auxiliary electrode and a thermocouple of the ISA type K (chromel-alumel junction) were placed in the outside compartment containing a molten binary salt mixture.

The cell was found very satisfactory for the study of the effect of diluents such as sodium ions which were coulometrically added to the cathode depolarizer by ionic conduction through the ceramic.

2.2 EXPERIMENTAL RESULTS

The evaluation of cathode materials was performed by measuring the open circuit potential and the polarized potentials at current densities of 0.015 amp/cm^2 and 0.150 amp/cm^2 of cathode area as a function of time.

The potentials were measured using a Ag-0.13 m AgCl in LiCl-KCl reference electrode. All potentials, though, are reported with respect to a Ag-1 m AgCl in LiCl-KCl electrode. Various diluent were used during the reporting period. Initially calcium was the proposed anode material therefore the diluent was $CaCl_2$. The first liquid anode to be proposed was lithium and LiCl was then used as a diluent. When the use of lithium was eliminated because of its reactivity, Na anodes with NaCl as the diluent were considered (See Section 3).

2.2.1 COPPER (I)

When testing molten CuCl, potential shifts caused by the reduction of cupric ion initially present in the melt and generated at the anode of the test cell were repeatedly observed. A glass wool plug about 1/2 inch in length was inserted between the lower end of the graphite anode and the openings of the Pyrex sheath. This reduced markedly the diffusion of cupric ions from the anode and gave relatively more stable potentials under current drains.

Molten CuCl gave an initial open circuit potential of + 1.10 volts on gold electrodes and + 1.15 volts on tungsten electrodes at 500°C. At a current drain of 0.150 amp/cm^2 of cathode area, the potentials were + 0.38 volt and + 0.41 volt on gold and tungsten, respectively.

A mixture composed of equimolar concentration of CuCl and LiCl gave the following results.

Temperature	450°C	500°C
Initial Open Circuit Potential	+0.37V	+0.37V
Potential at 0.015 amp/cm^2	-	-0.19V
Potential at 0.150 amp/cm^2	-0.15V	-0.21V

Molten CuCl was further tested using the experimental cell shown in Figure 7 and described in the Section 2.1 of this report. In the initial experiments, a LiCl-KCl eutectic mixture was used in the anode compartment of the cell. The objective of this test was to transfer coulometrically lithium ions through the ceramic to the cathode compartment and evaluate the effect of this diluent on the depolarizing properties of the cathode material. The cathode of the Graphite/LiCl-KCl/Ceramic/CuCl/W system gave an initial open circuit potential of + 1.14 volt at 450°C. The ceramic separator cracked within 10 minutes of the start of the test. Dilution of the cathode depolarizer with the LiCl-KCl eutectic mixture ensued prematurely. To ascertain that the failure of the ceramic tube was caused by ionic stress rather than thermal shock, an identical experimental setup was heated gently to 450°C and allowed to remain an open circuit for about 1/2 hour before applying any current. A break of the ceramic occurred after passing a current of 5 ma for 8 minutes followed by a current drain of 50 ma for about 5 minutes was passed through the cell. Apparently the ceramic was not able to exchange sodium ions with lithium and/or potassium ions at the rates determined by the current used in the experiment.

No apparent physical stress or weakening of the ceramic was observed at the conclusion of a 72 hour test with the same experimental arrangement using molten $AlCl_3$-NaCl as anolyte. The cell was run at 450° in alternate periods of 54 minutes at low current drain (0.015 amp/cm^2 of cathode area) and six minutes at high current drain (0.150 amp/cm^2). The results of the test is shown in Figure 8. It must be noted that the graph shows plottings of a single run and represents sequent potentials at high and low current drains.

Assuming Faraday's Law was obeyed and a coulometric transfer of sodium ions into the cathode compartment of the cell occurred, one-third of the initial amount of CuCl was left in the cathode compartment and the equivalent ratio between the remaining CuCl and NaCl was 1 to 2 at the conclusion of the 72 hour test.

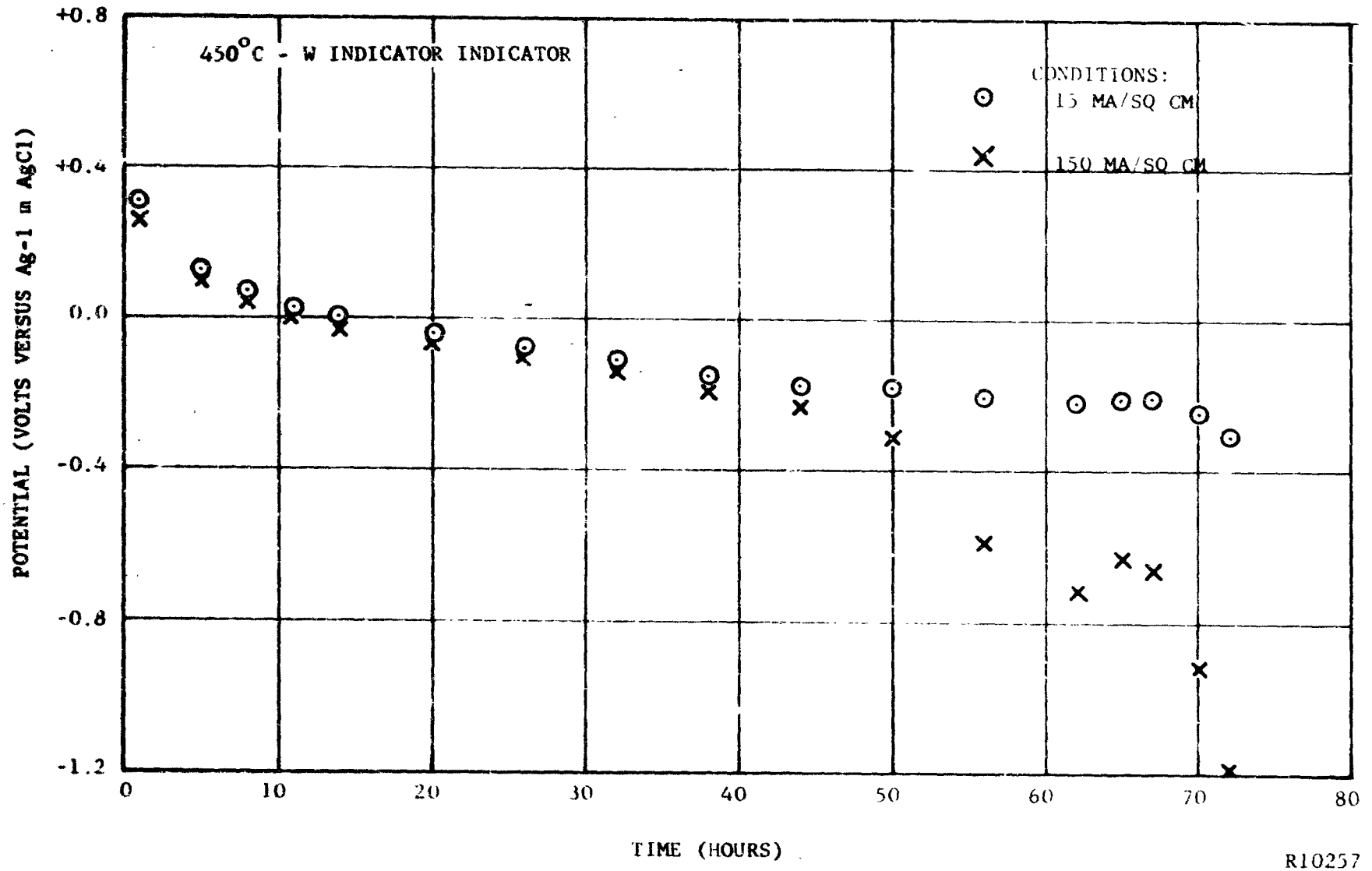

FIGURE 8. CuCl REDUCTION - COULOMETRIC ADDITION OF Na^+ 72 HOURS

A Na/Ceramic/CuCl cell was assembled as shown in Figure 9 in order to evaluate the compatibility of the ceramic having the composition shown above with liquid sodium and CuCl melt and to obtain other pertinent informations on the behavior of the galvanic couple at 450-500°C. About 1 g of sodium and 3 g of CuCl were used. The open circuit of the cell, initially at 3.675 volts, stabilized at 3.640 volts. The anode potential was -2.530 volts and the cathode potential was + 1.110 volts with respect to Ag - 1m AgCl reference electrode at 450°C. The internal resistance of the cell as measured with an a.c. conductivity bridge was 197 ohms at 450°C and 125 ohms at 480°C. The performance of this cell was determined by loading with a variable resistor and the resulting cell voltage was measured. The cell voltage stabilized at a fixed value within two minutes after the load resistor was changed. The characteristics of the cell are given in Table XV.

The cell was allowed to remain on open circuit for about three hours before it was dismantled for examination. No evidence of ceramic deterioration or stress was observed on the surface exposed to the cathode depolarizer. The internal side of the ceramic tube in contact with liquid sodium was observed to have been blackened. In spite of this apparent chemical attack and some diffusion of the sodium into the ceramic, the open circuit voltage and the internal resistance of the cell remained practically unchanged.

2.2.2 COPPER (II)

Gold, tungsten and graphite were used as electrode materials in $CuCl_2$ at 525°C. The gold electrodes dissolved completely within ten minutes following their immersion in the molten salt. The tungsten electrodes were found satisfactory for tests lasting up to several hours although substantial dissolution of the metal occurred. A spectroscopic graphite rod having a density of 1.90 g/cm^3 was found to have expanded and softened as a result of about one hour immersion in $CuCl_2$ melt.

Gold electrodes were also used in solutions composed of $CuCl_2$ and LiCl-KCl eutectic mixture. The dissolution of gold was not significantly reduced in these solutions in spite of the reduction in electrochemical activity which is shown in Table XVI.

Some effort was expended to find a suitable cathode material for use in $CuCl_2$ melt. The selected electrode materials include tantalum, tungsten, pyrolytic graphite, boron carbide and "Glassy Carbon". The results were as follows:

1. A tantalum wire 50 mils in diameter completely dissolved within 15 hours in the melt at 525°C.

2. A tungsten wire 25 mils in diameter partially dissolved under the same conditions.

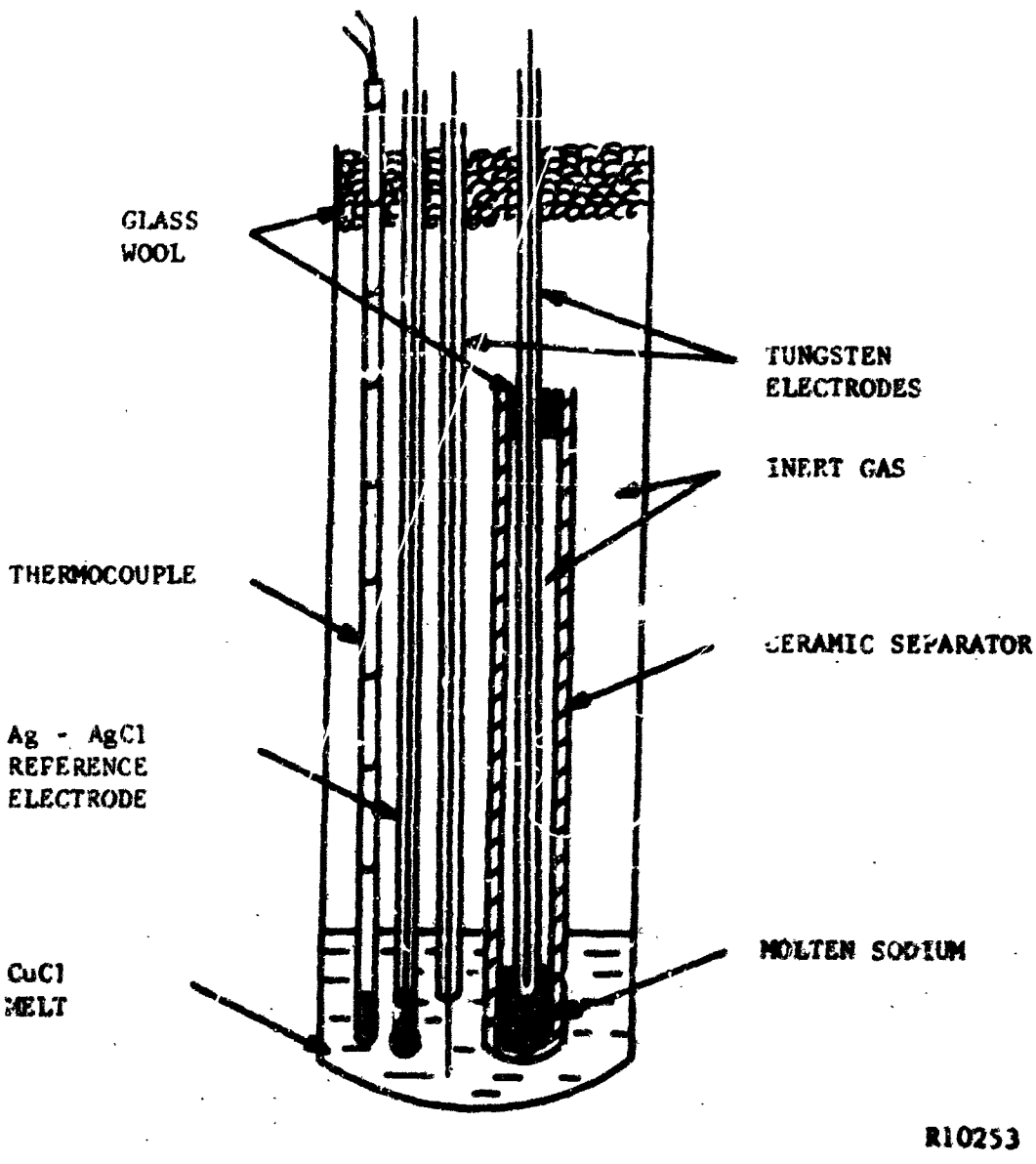

FIGURE 9. EXPERIMENTAL CELL

TABLE XV

PERFORMANCE CHARACTERISTICS OF NA/CERAMIC/CuCl CELL

Load Resistance (ohm)	Cell Voltage (volt)	Calculated Current (ma)
∞	3.64	0
900	2.94	3.3
600	2.68	4.5
400	2.37	5.9
200	1.765	8.8
100	1.172	11.7
50	0.705	14.1
20	0.315	15.8
10	0.160	16.0

TABLE XVI

CHARACTERISTICS OF $CuCl_2$ CATHODES

Depolarizing Solution	Temperature (°C)	Electrode Material	Open Circuit Potential vs. Ag-1mAgCl ref. electrode	Polarization at 0.015 amp/cm^2	Polarization at 0.150 amp/cm^2
$CuCl_2$	525	Tungsten	+ 1.39V	-	0.02V
$CuCl_2$	525	Graphite	+ 1.44V	-	-
$CuCl_2$	525	Gold	+ 1.39V	-	0.03V
50 mole % $CuCl_2$ 50 mole% LiCl-KCl eutectic mixture	450	Gold	+ 0.88V	0.01V	0.05V
25 mole% $CuCl_2$ 75 mole % LiCl-KCl eutectic mixture	450	Gold	+ 0.78V	0.01V	0.12V

3. A sample of pyrolytic graphite held in molten $CuCl_2$ at 540°C for 15 hours expanded in the direction perpendicular to the plane of deposition.

4. A rod section of "Glassy Carbon" (from the Tokai Electrode Mfg. Co. in Tokyo, Japan) dissolved to about 2/3 of its initial size in $CuCl_2$ melt at 540° for 72 hours. The remaining part of the rod section retained the glossy appearance and strength observed before treatment.

5. Boron Carbide (supplied by the Norton Company) was found unattacked following immersion in the melt at 540°C for 72 hours.

The specific resistivities of boron carbide and "Glassy Carbon", determined in the temperature range between 25° and 525°C by means of a four point probe, are given in Table XVII. The sample of boron carbide used in the experiment was a 1/4 inch rod having the following composition:

B	76.5% min.
C	20-22% min.
B_2O_3	0.2% min.
Fe	0.5% max,
Al	0.2% max.
Ca	0.1% max.
Mg	0.05% max.

Because of the difficulties associated with finding suitable materials to contain the highly oxidizing $CuCl_2$ no further tests were run using this depolarizer.

TABLE XVII

SPECIFIC RESISTIVITY OF BORON CARBIDE AND "GLASSY CARBON"

Boron Carbide		"Glassy Carbon"	
Temperature °C	Specific Resistivity ohm-cm	Temperature °C	Specific Resistivity ohm-cm
25	0.398	27	4.900×10^{-3}
100	0.204	114	4.754×10^{-3}
150	0.143	202	4.626×10^{-3}
197	0.105	292	4.501×10^{-3}
300	0.061	396	4.382×10^{-3}
400	0.040	524	4.186×10^{-3}
52[illegible]	0.022		

2.2.3 BISMUTH (III)

Pure molten $BiCl_3$ and a mixture of $BiCl_3$, $CaCl_2$ and Bi^o were tested using the cell arrangement shown in Figure 8 in the First Quarterly Report(1). The results can be summarized as follows:

Depolarizing Solution	Temperature (°C)	Electrode Material	Open Circuit Potential	Polarization at 0.015 amp.cm^2	0.150 amp/cm^2
$BiCl_3$	425	Tungsten	+ 0.92 V	0.03 V	0.1 V
$BiCl_3$ 2 equiv. $BiCl_2$ 1 equiv. Bi 1 equiv.	425	Tungsten	+ 0.40 V	0.01 V	0.1 V
		Gold	+ 0.46 V	0.015 V	0.1 V

The potential time curves for these systems are shown in Figure 10.

The deterioriation of the gold electrode in the ternary mixture became evident within 15 minutes after the start of the test as the potential became erratic and a rapid increase in polarization occurred. The failure of the electrode was attributed to the formation of a molten Bi-Au alloy. No evidence of chemical attack was observed on the tungsten electrode at the conclusion of the test.

Two experiments were performed with Graphite/Ceramic/$AlCl_3$·NaCl/Ceramic/$BiCl_3$ cells using the experimental arrangement shown in Figure 7. The cells were operated at a temperature of 380°C. Based on a 2-electron reduction to BiCl and cycling current densities of 0.150 amp/cm^2 of cathode area for 6 minutes and 0.015 amp/cm^2 for 54 minutes every hour for 72 hours, an amount of $BiCl_3$ 50% in excess of the theoretical amount was used. The first test was concluded after 72 hours while the second test was allowed to continue until substantial polarization and instability in the system was noted. This occurred after 115 hours. Figures 11 and 12 show the results of these tests. The relatively high potential differences between low and high current drains shown in Figure 11 were caused by a large IR drop between the indicator electrode and the reference electrode which has been inadvertently placed too far from the cathode. It appears from the performance of the second cell that directly or indirectly, a 3-electron reduction of Bi^{+++} to Bi^o has occurred. This was substantiated by the presence of bismuth metal in the cathode compartment of the cell at the conclusion of the experiment.

Again the ceramic separators were found to be intact after these tests.

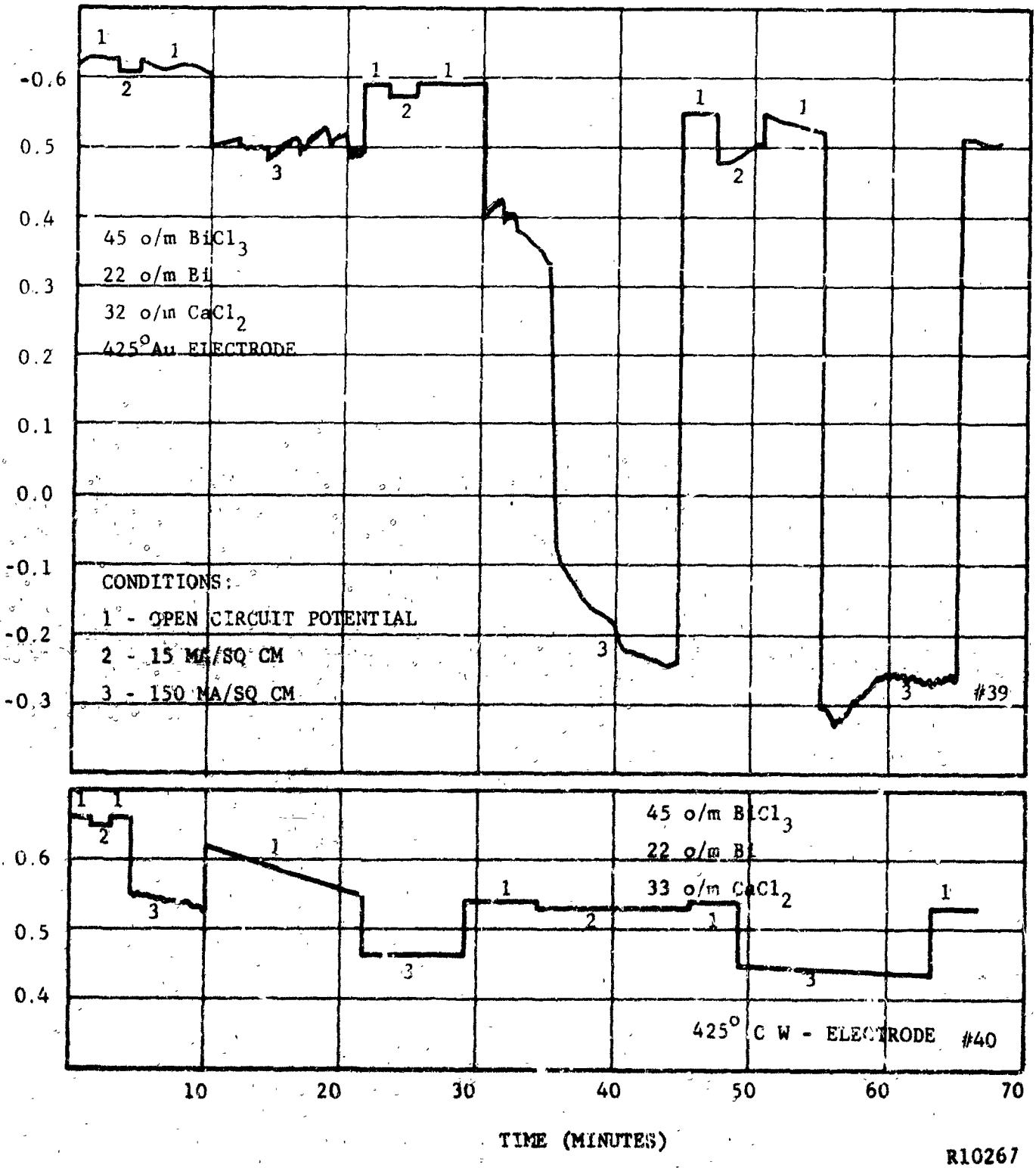

FIGURE 10. $BiCl_3$ REDUCTION. EFFECT OF DILUENT AND ELECTRODE

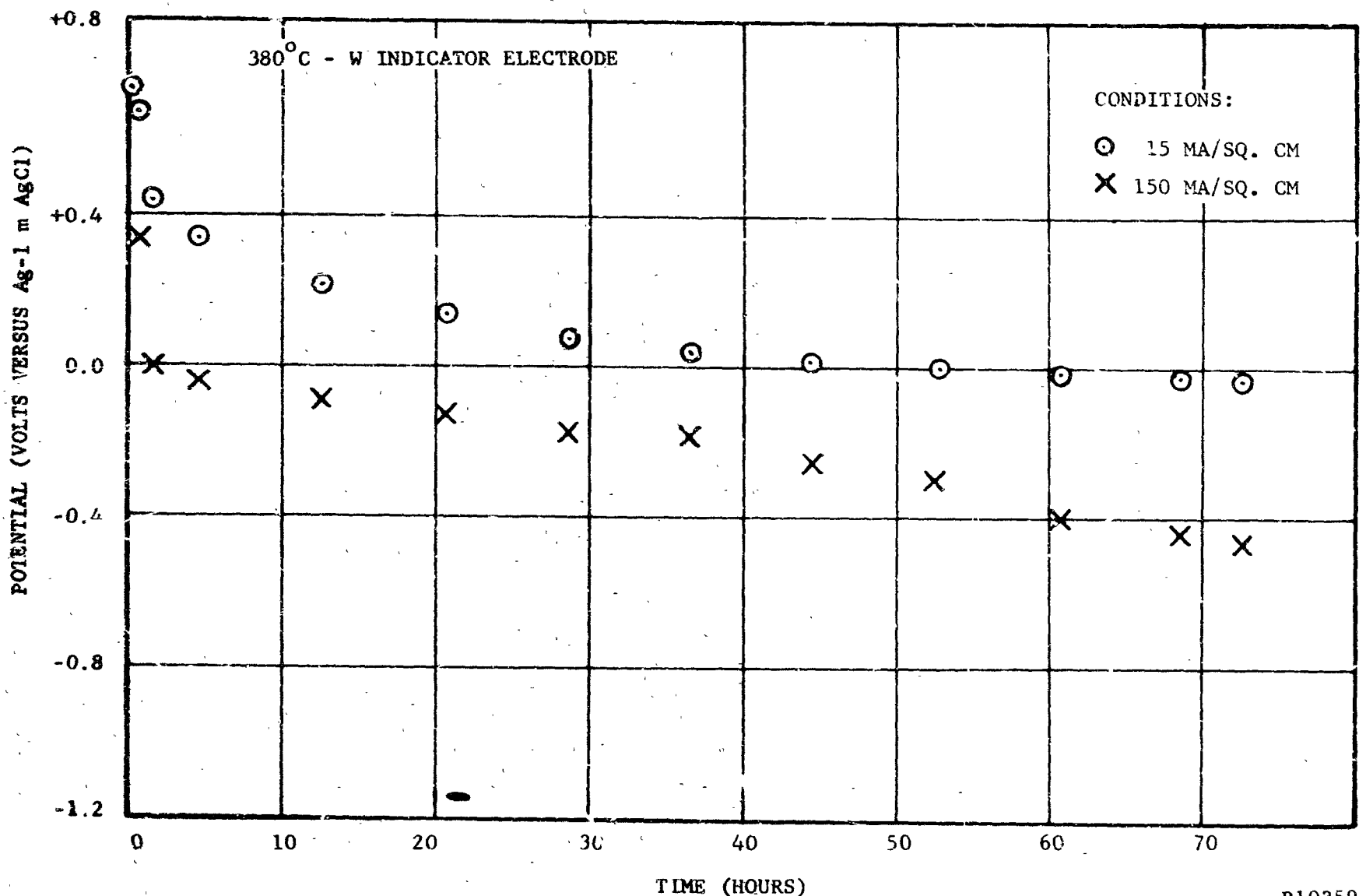

FIGURE 11. $BiCl_3$ REDUCTION EFFECT OF DILUENT COULOMETRIC ADDITION OF Na^+. 72 HOURS

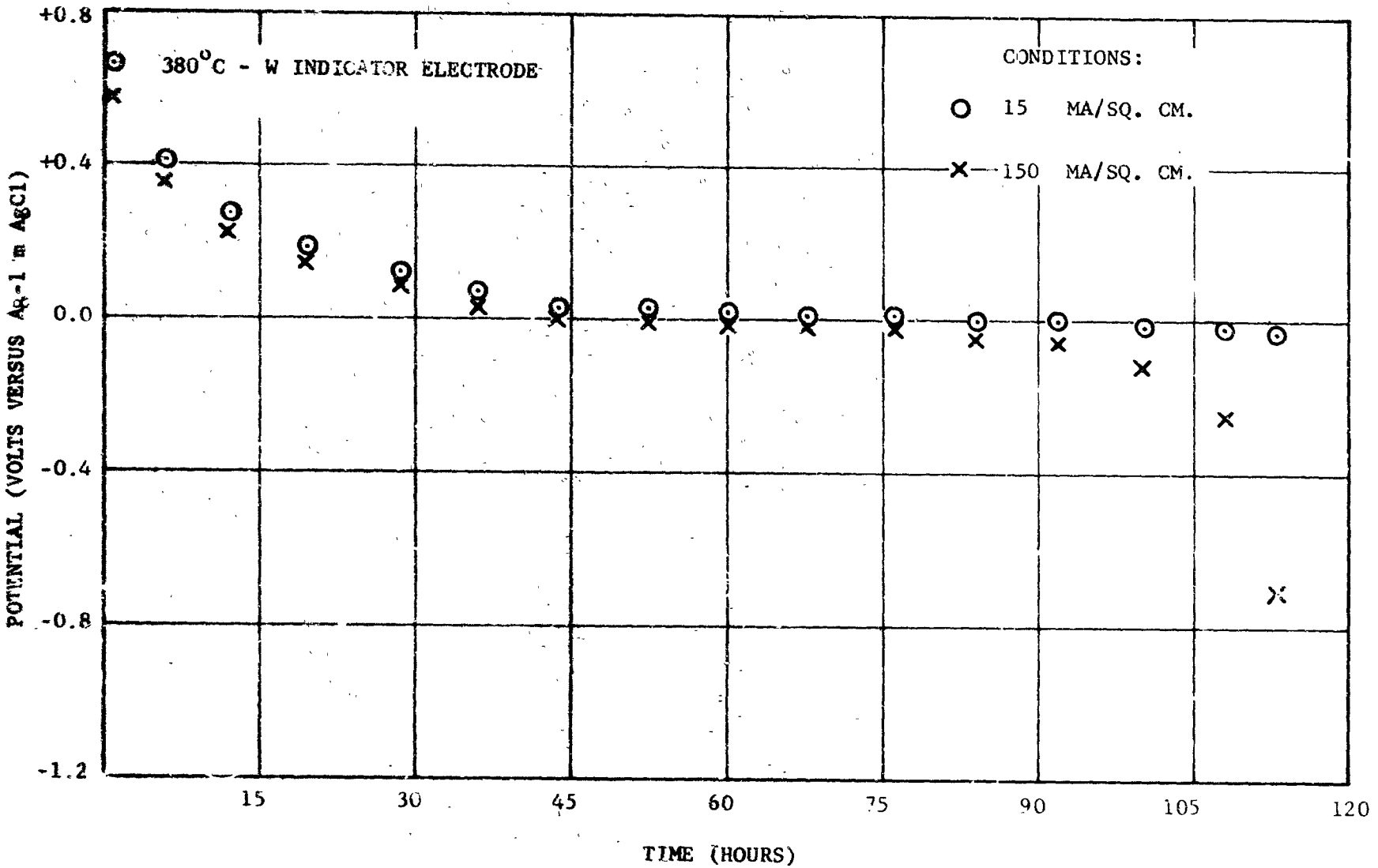

R10258

FIGURE 12. $BiCl_3$ REDUCTION. EFFECT OF DILUENT-COULOMETRIC ADDITION OF Na^+. 115 HOURS

2.2.4 IRON (III)

Gold electrodes were used in solutions composed of 1 mole of $FeCl_3$ in 4.5 moles of LiCl-KCl eutectic mixture (mean molecular weight = 55.59), and 1/3 mole $FeCl_3$ plus 1/2 mole $CaCl_2$ in 3 moles of the eutectic mixture at 450°C. Open circuit potentials and polarizations at 0.015 and 0.150 amp/cm^2 of cathode area were, respectively, + 0.70 volt, 0.03 volt and 0.1 volt in the first solution and + 0.65 volt, 0.05 volt and 1.3 volts in the solution containing $CaCl_2$; respectively.

Equimolar quantity of $FeCl_3$ and LiCl-KCl eutectic mixture gave an open circuit potential of + 0.73 volt at 450°C on a tungsten electrode. Polarizations at 0.015 amp/cm^2 and 0.150 amp/cm^2 of cathode area were 10 to 15 mv and about 1.2 volts, respectively. Experimental curves for these systems are given in Figure 13. Compositions are given in mole percent. The potential scale given in this figure is with respect to a Ag-0.13 m AgCl electrode which was used as a reference electrode. To convert these potentials to the Ag-1m AgCl scale, 0.127 volt must be subtracted from those given in the figure. The large polarization observed at the higher current drain was attributed to the local depletion of ferric ions in the vicinity of the indicator electrode resulting in transition from the Fe(III)-Fe(II) system to the Fe(II)-Fe(0) system.

2.2.5 SILVER (I)

The open circuit potential of a gold electrode in a solution composed of 85 mole percent of AgCl and 15 mole percent of $CaCl_2$ at 500° was +0.31 volt. The polarization was less than 30 mv at 0.150 amp/cm^2 of cathode area. Potential-time curve for this system is shown in Figure 14.

2.3 CERAMIC ION EXCHANGE

In an effort to coulometrically add Li^+ to the cathode depolarizers without cracking the ceramic separator, efforts were made to exchange the Na^+ of the ceramic with Li^+. Exchange of sodium ions for lithium ions in ceramic tubes having the composition given in Section 2.1 of this report was performed by immersing the tubes in molten lithium nitrate at 285°C for 8 days. The tubes were 170 mm long and 10.5 mm in outside diameter. The melt was replenished every other day with a fresh batch. Following this treatment the tubes were rinsed with water and dried in vacuum at 300°C. Two of these tubes were again filled with lithium nitrate melt and partially immersed in more of the melt at 300°C. By means of graphite electrodes inserted in the tubes, current drains of 50 ma and 100 ma were passed through the ceramic for one hour in alternate periods of about 10 minutes. No visible evidence of stress was observed on the ceramic. The tubes were again rinsed and dried then given the

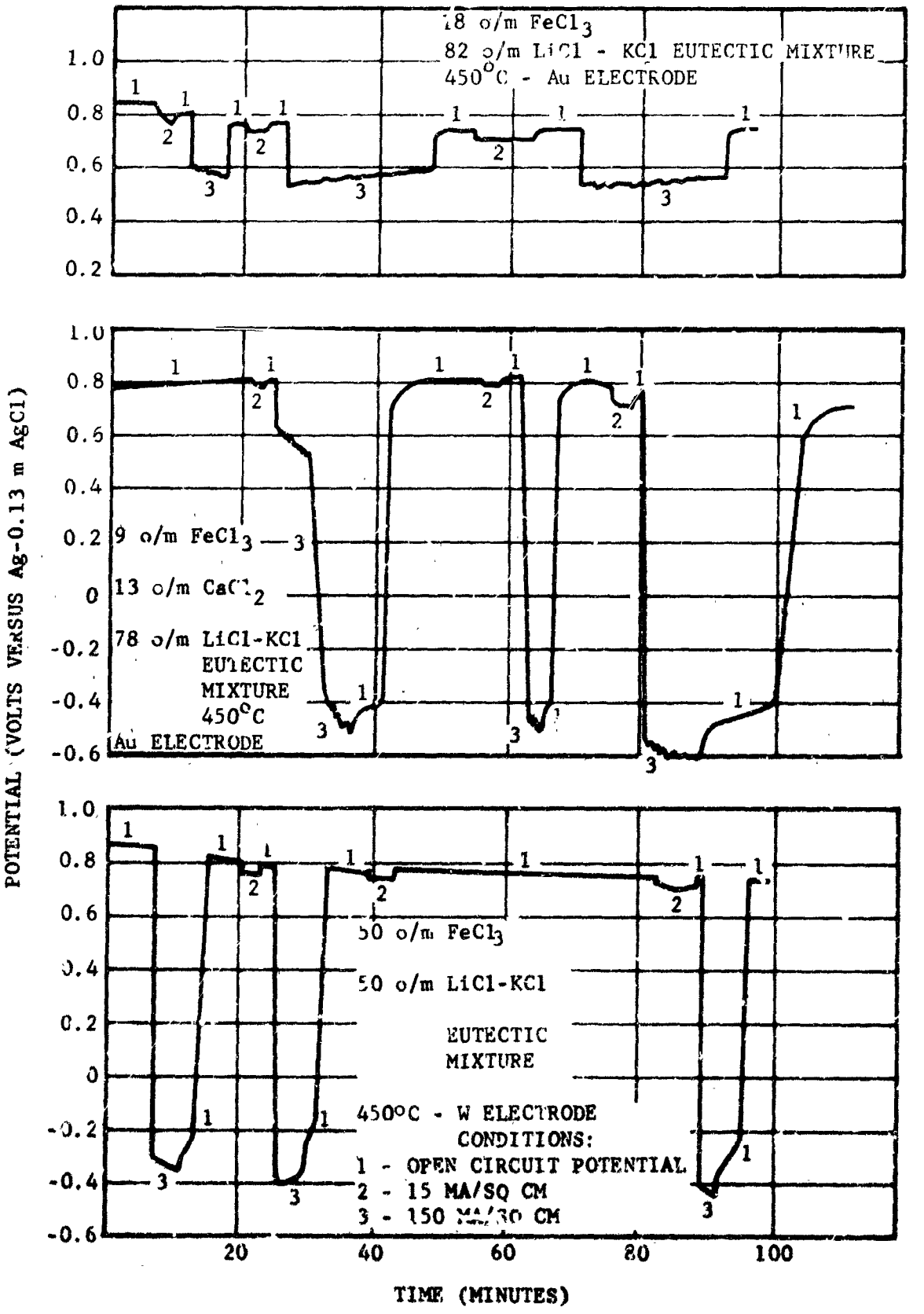

FIGURE 13. $FeCl_3$ REDUCTION. EFFECT OF DILUENT AND ELECTRODE

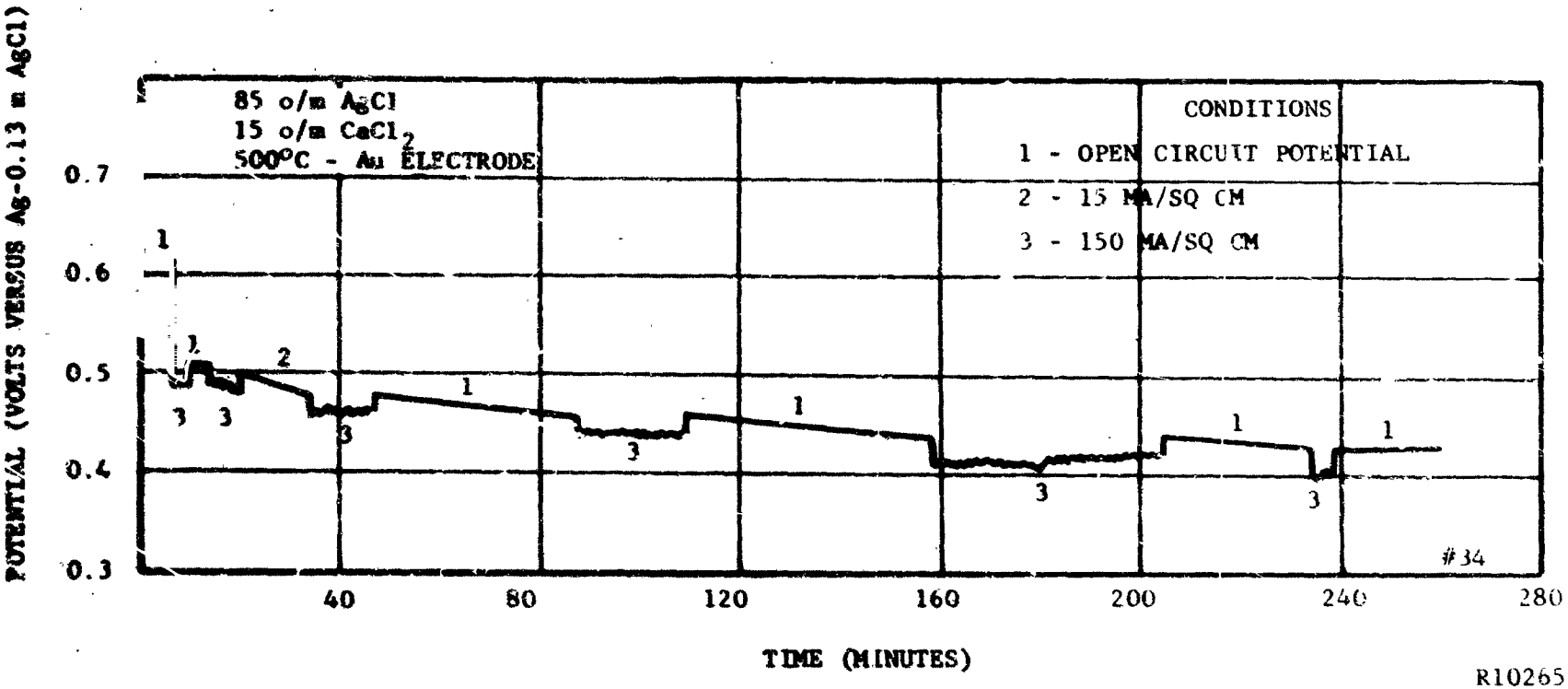

FIGURE 14. AgCl REDUCTION. EFFECT OF DILUENT

same galvanic treatment using LiCl-KCl eutectic mixture, in place of $LiNO_3$, at 450°C. The ceramic tubes showed marked crazing throughout the area that was immersed in the eutectic mixture. This was probably caused by stresses from uneven exchange with lithium ions and potassium ions in the ceramic.

SECTION 3

ANODE STUDIES

Calcium metal was first proposed as the anode for this cell. This selection was predicated by the low equivalent weight and highly reducing nature of calcium. However further consideration of this anode material lead to the conclusion that problems associated with maintaining electrical contact between the solid zeolite electrolyte and solid calcium was difficult to overcome. This problem is intensified in this application where a considerable amount of the anode material is consumed during cell discharge. Consequently solid calcium anodes were dropped from consideration, and attention focused upon anode materials which would be liquid at the cell operating temperature.

Lithium, by reason of its low equivalent weight, was the first liquid anode to be considered. However the corrosive nature of molten lithium as shown in compatibility tests (Section 4.3) eliminated the use of lithium in the present application.

Sodium was next considered as the anode material. One of the determining factors in this selection is the wealth of information on the technology and properties of liquid sodium (8). Experimental results of a cell of the type

Na/Ceramic/CuCl

are given in Section 2.2.1 and results of compatibility tests with molten sodium are given in Section 4.3

SECTION 4

CELL CONSTRUCTION

In anticipation of assembly and testing of complete cells and batteries, a preliminary cell design was formulated in an attempt to determine areas in which special problems might arise.

4.1 CELL VOLUME CHANGES

One of the first points which must be taken into account in the design of a cell for this application is the change in volume which will occur during discharge. Using a zeolite as a solid electrolyte permitting only cation transfer between the anode and cathode compartment results in a decrease in volume in the anode compartment and an increase in volume in the cathode compartment. In the anode compartment the active metal anode is oxidized to form ions. The transfer of these ions as the charge carriers through the zeolite results in a net volume decrease in the anode compartment. In the cathode compartment there is a volume change due to the reduction of the cathode material from one oxidation state to a lower one and the introduction of cations from the anode compartment through the zeolite.

As an example of the volume changes to be encountered consider a cell composed of a sodium anode and a CuCl cathode. The individual half reactions expected are:

$$\text{Anode} \qquad Na \longrightarrow Na^{+} + 1e^{-}$$

$$\text{Cathode} \qquad CuCl + 1e^{-} \longrightarrow Cu + Cl^{-}$$

with one Na+ passing from the anode compartment through the zeolite membrane to the cathode compartment for each electron transferred.

For a total capacity of 14 ampere-hour, the amount of metallic sodium oxidized, sodium ion transferred, and CuCl reduced are each 0.523 faradays. The loss of 0.523 faradays (12.0 grams) of metallic sodium is equivalent to a volume decrease at 450°C of

$$\frac{12.0 \text{ grams}}{0.842 \text{ grams/cm}^3} = 14.25 \text{ cm}^3$$

The density of molten sodium was calculated from data given in reference 8. The situation in the cathode compartment is more complex since there is a transformation of 0.523 equivalents of CuCl to Cu and the introduction of 0.523 equivalents of NaCl. Assume that CuCl and NaCl from ideal solution; i.e., their individual volume are additive, and that the volume of NaCl dissolved in CuCl can be extrapolated from the high temperature molten volumes of NaCl. Then the decrease in volume of CuCl is,

$$0.523 \text{ equiv.} \times \frac{98.99 \text{ grams}}{\text{equiv.}} \times \frac{\text{cm}^3}{3.655 \text{ grams}} = 14.16 \text{ cm}^3$$

The volume increase due to formation of Cu is

$$0.523 \text{ equiv.} \times \frac{63.54 \text{ grams}}{\text{equiv.}} \times \frac{\text{cm}^3}{8.73 \text{ grams}} = 3.81 \text{ cm}^2$$

and the formation of NaCl is

$$0.523 \text{ equiv.} \times \frac{59.44 \text{ grams}}{\text{equiv.}} \times \frac{\text{cm}^3}{1.746 \text{ grams}} = 17.81 \text{ cm}^3$$

The densities of CuCl and NaCl at 450°C were obtained from reference 9. The density of Cu at 450° was calculated from its known density at 0°C and its coefficient of thermal expansion. Thus the total volume change in the cathode compartment is

$$-14.16 + 3.81 + 17.81 = 7.46 \text{ cm}^3$$

Similar calculations show that using a potassium anode the volume of the anode section would decrease 27.8 cm^3 while the cathode section would increase 12.4 cm^3. The results for these two systems are summarized in Table XVIII.

TABLE XVIII

VOLUME CHANGES IN 14 AMPERE-HOUR CELL

	Volume Change, cm^3		
Cell	Anode	Cathode	Cell
Na/Zeolite/CuCl	-14.25	+7.46	-6.79
K/Zeolite/CuCl	-27.8	+12.4	-15.4

4.2 CELL DESIGN

To accommodate these volume changes, a preliminary cell design utilizing movable bellows as containers for the anode and cathode sections was formulated. This preliminary design is shown in Figure 15. The bellows would be fabricated from Armco iron, nickel, or stainless steel. It would appear from preliminary information that molybdenum-manganese ceramic to metal seals utilizing iron or nickel brazing alloys would have the best change of surviving in contact with the liquid metal anode. Glass sealants, e.g., pyroceramic types or sodium phosphate glass, would be usable in this configuration since they are not in contact with the liquid anode.

4.3 COMPATIBILITY TESTS

Compatibility tests were run for various materials proposed for use in cell construction. In these tests the materials were vacuum sealed in Pyrex ampoules. The tests were run by holding the materials in contact with each other at 450°C for a minimum of 72 hours. In most cases visual examination was used to determine changes.

Molten lithium was found to severely attack recrystallized alumina by destroying its structural integrity. In addition, some etching of the glass container by lithium distilled from the original sample was noted. Lithium is said to be one of the most corrosive of the liquid metals.[8] Because of the difficulties associated with handling liquid lithium and the time involved in developing the required technology, no further work was done on systems utilizing lithium anodes. In addition, the lithium ion, because of its smaller size, is held with greater coulombic attraction to the sites of negative charge present in the zeolite lattice. This greater attraction is apparent in the higher resistivity and activation energy for conduction found with lithium zeolites (see Section 1.3.1).

Samples of the sodium zeolites, Types A, X, and Y, and Armco iron, nickel, and recrystallized alumina were exposed to molten sodium for 72 hours at 450°C. The zeolites appeared to be penetrated by the molten sodium. This was evidenced by a yellow coloration extending a few millimeters into the zeolite pellets. After exposure to molten sodium, zeolite pellets reacted with water to liberate hydrogen. The mechanism of this penetration is not known but it is possibly through pores or channels of the zeolite crystallite. It is these channels which give synthetic zeolites their molecular sieve properties. If penetration is by way of these pores, it may be eliminated or minimized by blocking the pores with a solid or liquid material.

No apparent reaction was noted between molten sodium and Armco iron, nickel, or recrystallized alumina. It would appear that these materials are suitable for use in the proposed cell.

Sodium zeolites, Types A, X, and Y were checked for compatibility with molten CuCl, molten $BiCl_3$, and LiCl-KCl eutectic. In addition, Armco iron, nickel, and Al_2O_3 were checked in the same molten salts. No apparent reaction was noted between the zeolites and the molten salts. Some penetration of the molten LiCl-KCl

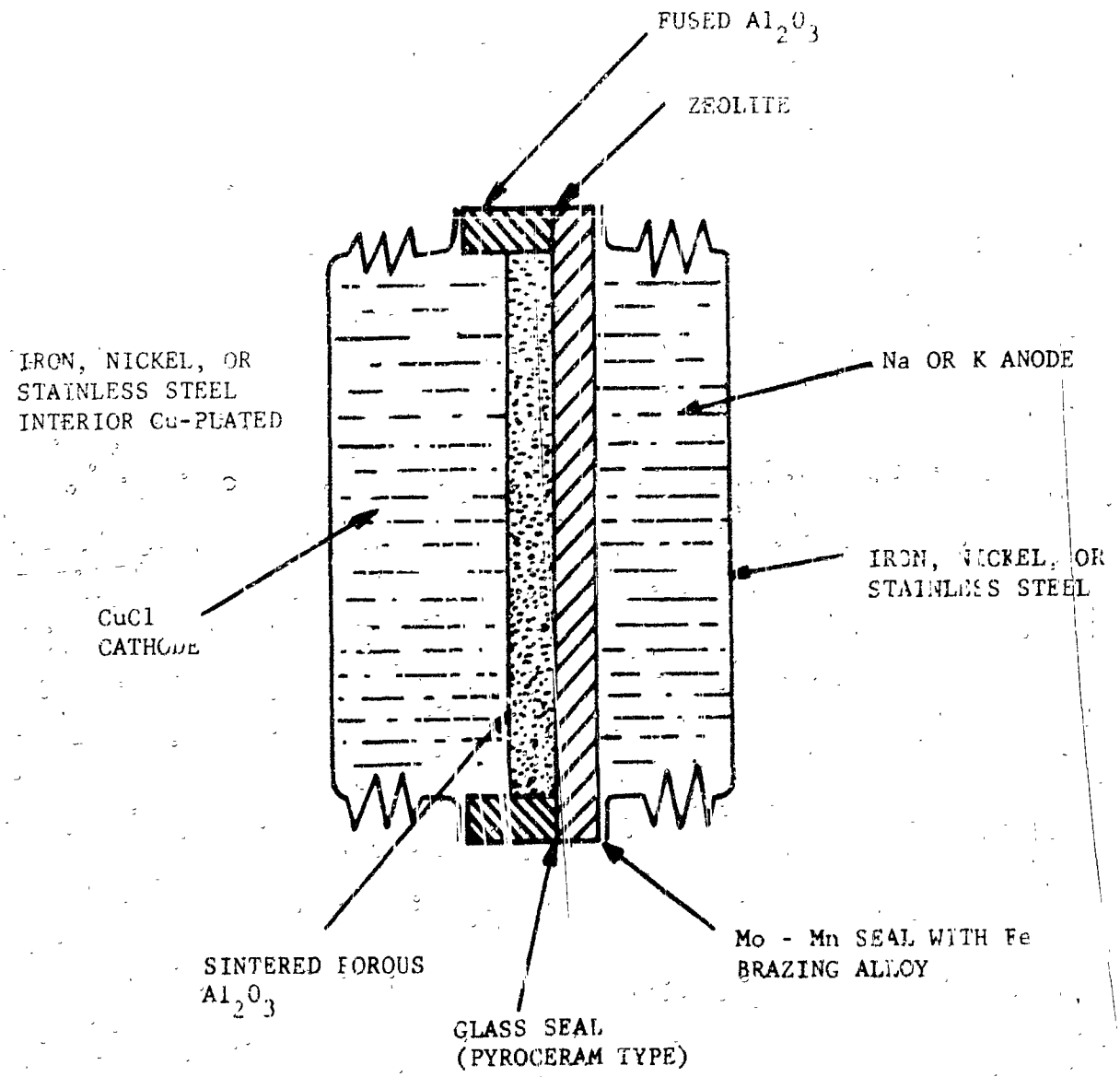

FIGURE 15. PRELIMINARY CELL DESIGN

in the zeolite appeared to occur. This conclusion is based upon an apparent decrease in volume of the molten salt. In the tests involving CuCl, a black residue was noted at the end of the test period. However, there are reports that CuCl does turn dark in the presence of light. This could be due to a photo-decomposition of CuCl to form finely divided copper,

$$CuCl \longrightarrow Cu + 1/2\ Cl_2$$

similar to the photo-decomposition of AgCl.

Molten LiCl-KCl did not react with Armco iron, nickel, or Al_2O_3. Molten CuCl did not react with Ni or Al_2O_3. It did react with Armco iron to form an adherent coating of metallic copper. The reaction was probably

$$2Cu^{+} + Fe \longrightarrow 2Cu + Fe^{+}$$

Molten $BiCl_3$ did not react with Al_2O_3, but it did react with Ni and Fe. Unlike the results with CuCl, no adherent deposit of Be was obtained. Bi, formed by the reaction,

$$2Bi^{+++} + 3Ni \longrightarrow 2Bi + 3Ni^{++}$$

is very soluble in molten $BiCl_3$. The phase diagram for the $BiCl_3$-Bi system shows that at these temperatures the solubility of Bi in $BiCl_3$ is about 30 mole per cent. Thus, the Bi plated on the Ni or Fe immediately dissolves in $BiCl_3$ and thus leaves a surface of Ni or Fe for further reaction. Cu, on the other hand, has a very, very low solubility in molten CuCl, so a protective layer is formed.

SECTION 5

FUTURE WORK

Efforts will be concentrated on developing a satisfactory membrane with a decreased porosity and to develop techniques to fabricate and test complete cells. In the area of membranes, methods of filling the zeolite pores with a suitable material, e.g., LiCl-KCl eutectic, will be investigated while coulometrically passing sodium ions through the membranes. Membrane bonding techniques will be modified to permit fabrication of large diameter thin membranes. The goal is a membrane 2 inches in diameter and 10 to 15 mils thick.

Investigations of compatibility of proposed components will continue. Cell bonding and fabrication techniques will be studied and directed towards the production of complete cells suitable for testing. A suitable chamber and electronic equipment for cell and battery testing in a simulated Venus atmosphere will be assembled.

REFERENCES

1. Aeronutronic Division, Philco Corporation, First Quarterly Report, Contract NAS3-6002, NASA Report No. CR-54202, October 1964.

2. C. L Clark, Applied X-rays, Fourth Edition, McGraw-Hill Co., Inc., New York, pp. 420-2 (1955).

3. D. W. Breck, W. G. Eversole, R. M. Milton, T. B. Reed, and T. L. Thomas, J. Amer. Chem. Soc. 78, 5963 (1956).

4. R. M. Milton, U. S. Patent 2,882,244, April 14, 1959.

5. Union Carbide Corp. (by D. W. Breck), German Patent 1,098,929, April 14, 1958.

6. DMIC Report 169, "The Effect of Molten Alkali Metals on Containment Metals and Alloys at High Temperatures," May 28, 1962.

7. R. J. Labrie, J. Electrochem. Soc. 111, 473 (1963).

8. Richard N. Lyon, Liquid-Metals Handbook, Second Edition, June 1962.

9. Milton Blander, Editor, Molten Salt Chemistry, Interscience Publishers, New York (1964).

DISTRIBUTION

National Aeronautics and Space Administration
Washington D. C. 20546

Attn: Miss Millie Ruda, Code AFSS-LD
3 Copies

National Aeronautics and Space Administration
Washington D. C. 20546

Attn: Walter C. Scott, Code RP
1 Copy

National Aeronautics and Space Administration
Washington D. C. 20546

Attn: Ernst M. Cohn, Code RNW
1 Copy

National Aeronautics and Space Administration
Washington D. C. 20546

Attn: George F. Esenwein, Code MSA
1 Copy

National Aeronautics and Space Administration
Washington D. C. 20546

Attn: A. M. Andrus, Code FC
1 Copy

National Aeronautics and Space Administration
Washington D. C. 20546

Attn: J. R. Miles, Code SL
1 Copy

National Aeronautics and Space Administration
Washington D. C. 20546

Attn: Welfred M. Redler, Code PE
1 Copy

National Aeronautics and Space Administration
Goddard Space Flight Center
Greenbelt, Maryland

Attn: Thomas Hennigan, Code 632.2
1 Copy

National Aeronautics and Space Administration
Goddard Space Flight Center
Greenbelt, Maryland

Attn: Joseph Shirfey, Code 652
1 Copy

National Aeronautics and Space Administration
Goddard Space Flight Center
Greenbelt, Maryland

Attn: Paul Donnelly, Code 636.2
1 Copy

National Aeronautics and Space Administration
Lewis Research Center
21000 Brookpark Road
Cleveland, Ohio 44135

Attn: N. D. Sanders MS 302-1
1 Copy

National Aeronautics and Space Administration
Lewis Research Center
21000 Brookpark Road
Cleveland, Ohio 44135

Attn: Martin J. Saari MS 500-201
1 Copy

DISTRIBUTION (Continued)

National Aeronautics and Space Administration
Lewis Research Center
21000 Brookpark Road
Cleveland, Ohio 44135

Attn: Robert L. Cummings MS 500-201
1 Copy

National Aeronautics and Space Administration
Lewis Research Center
21000 Brookpark Road
Cleveland, Ohio 44135

Attn: Harvey J. Schwartz MS 500-201
1 Copy

National Aeronautics and Space Administration
Lewis Research Center
21000 Brookpark Road
Cleveland, Ohio 44135

Attn: J. J. Weber MS 15-1
1 Copy

National Aeronautics and Space Administration
Lewis Research Center
21000 Brookpark Road
Cleveland, Ohio 44135

Attn: J. E. Dilley MS 500-309
1 Copy

National Aeronautics and Space Administration
Lewis Research Center
21000 Brookpark Road
Cleveland, Ohio 44135

Attn: B. Lubarsky MS 500-201
1 Copy

National Aeronautics and Space Administration
Lewis Research Center
21000 Brookpark Road
Cleveland, Ohio 44135

Attn: M. R. Unger MS 500-201
1 Copy
+ 1 Repro

National Aeronautics and Space Administration
Lewis Research Center
21000 Brookpark Road
Cleveland, Ohio 44135

Attn: Library
1 Copy

National Aeronautics and Space Administration
Lewis Research Center
21000 Brookpark Road
Cleveland, Ohio 44135

Attn: Report Control Office
Mail Stop 5-5 1 Copy

National Aeronautics and Space Administration
Scientific and Technical Information Facility
P. O. Box 5700
Bethesda 14, Maryland

Attn: NASA Representative
2 Copies
+ 1 Repro

National Aeronautics and Space Administration
Marshall Space Flight Center
Huntsville, Alabama

Attn: Richard Boehme, Bldg 4487-BB
M-ASTR-EC 1 Copy

National Aeronautics and
Space Administration
Manned Space Craft Center
Houston 1, Texas

Attn: William R. Dusenbury
Propulsion and Energy Systems
Branch
Energy Systems Division
Bldg 16, Site 1 1 Copy

National Aeronautics and
Space Administration
Manned Space Craft Center
Houston 1, Texas

Attn: Robert Cohen
Gemini Project Office
1 Copy

National Aeronautics and
Space Administration
Manned Space Craft Center
Houston 1, Texas

Attn: Richard Ferguson, EE-5
1 Copy

National Aeronautics and
Space Administration
Manned Space Craft Center
Houston 1, Texas

Attn: Forrest E. Eastman, EE-4
1 Copy

National Aeronautics and Space
Administration
Ames Research Center
Pioneer Project
Moffett Field, California

Attn: James R. Swain 1 Copy

Jet Propulsion Laboratory
4800 Oak Grove Drive
Pasadena, California

Attn: Yuji Echiyama 1 Copy

U. S. Army Engineer Research
and Development Labs
Fort Belvoir, Virginia 22060

Attn: Dr. Galen Frysinger
Electrical Power Branch
SMOFB-EP 1 Copy

U. S. Army Engineer Research
and Development Labs
Fort Monmouth, New Jersey

Attn: David Linden (Code SELRA/PS)
1 Copy

U. S. Army Research and Development
Liaison Group (9851 DV)
APO 757
New York, New York

Attn: B. R. Stein 1 Copy

Army Research Office
Office, Chief Research and Development
Department of the Army
3D 442, The Pentagon
Washington D. C. 20546

Attn: Dr. Sidney J. Magram
1 Copy

Harry Diamond Labs
Room 300, Bldg 92
Connecticut Avenue and
Van Ness Street, N. W.
Washington D. C.

Attn: Nathan Kaplan 1 Copy

Army Materiel Command
Research Division
AMCRD-RSCM T-7
Washington 25, D. C.

Attn: John V. Crellin 1 Copy

U. S. Army TRECOM
Fort Eustis, Virginia 23604

Attn: Dr. R. L. Echols
(SMOFE-PSG) 1 Copy

U. S. Army TRECOM
Fort Eustis, Virginia 23604

Attn: Leonard M. Bartone
(SMOFE-ASE)
Physical Sciences Group
Mechanical Systems Subgroup,
ASE 1 Copy

U. S. Army Research Office
Box CM, Duke Station
Durham, North Carolina

Attn: Paul Greer 1 Copy

U. S. Army Research Office
Box CM, Duke Station
Durham, North Carolina

Attn: Dr. Wilhelm Jorgensen
1 Copy

U. S. Army Mobility Command
Research Division
Center Line, Michigan 48090

Attn: O. Renius (AMSMO-RR)
1 Copy

Headquarters, U. S. Army
Materiel Command
Development Division
Washington 25, D. C.

Attn: Marshall D. Aiken
(AMCRD-DE-MO-P) 1 Copy

Office of Naval Research
Washington D. C. 20360

Attn: Dr. Ralph Roberts, Code 429
Head, Power Branch
1 Copy

Naval Research Laboratory
Washington D. C. 20390

Attn: Dr. J. C. White, Code 6160
1 Copy

Office of Naval Research
Department of the Navy
Washington D. C. 20360

Attn: H. W. Fox, Code 425
1 Copy

Bureau of Naval Weapons
Department of the Navy
Washington 25, D. C.

Attn: Whitwell T. Beatson
(Code RAAE-52) 1 Copy

Bureau of Naval Weapons
Department of the Navy
Washington 25, D. C.

Attn: Milton Knight (Code RAAE-50)
1 Copy

Bureau of Ships
Department of the Navy
Washington 25, D. C.

Attn: Bernard B. Rosenbaum
(Code 340) 1 Copy

Naval Ordnance Laboratory
Department of the Navy
Corona, California

Attn: Mr. William C. Spindle
(Code 441) 1 Copy

Naval Ordnance Laboratory
Department of the Navy
Silver Spring, Maryland

Attn: Philip B. Cole (Code WB)
1 Copy

Wright-Patterson AFB
Aeronautical Systems Division
Dayton, Ohio

Attn: ASRMFP-2/James Elsworth Cooper
1 Copy

AF Cambridge Research Lab
L. G. Hanscom Field
Bedford, Massachusetts

Attn: Commander (CRO) 1 Copy

Rome Air Development Center, ESD
Griffiss AFB, New York 13442

Attn: Commander (RAALD) 1 Copy

Headquarters, USAF (AFRDR-AS)
Washington 25, D. C.

Attn: Lt. Col. William G. Alexander
1 Copy

Capt William H. Ritchie
Space Systems Division
Air Force Unit Post Office
Los Angeles 45, California

Attn: SSZAE-11 1 Copy

Capt William Hoover
Air Force Ballistic Missile Division
Air Force Unit Post Office
Los Angeles 45, California

Attn: WDZYA-21 1 Copy

Mr. Charles F. Yost
Asst Director, Material Sciences
Advanced Research Projects Agency
The Pentagon, Room 3E 153
Washington 25, D. C 1 Copy

Dr. John H. Huth
Advanced Research Projects Agency
The Pentagon, Room 3E 157
Washington 25, D. C. 1 Copy

U. S Atomic Energy Commission
Auxiliary Power Branch (SNAP)
Division of Reactor Development
Washington 25, D. C.

Attn: LCOL George H. Ogburn Jr.
1 Copy

Lt. Col. John H. Anderson
Advanced Space Reactor Branch
Division of Reactor Development
U. S. Atomic Energy Commission
Washington 25, D. C. 1 Copy

Mr. Donald B. Hoatson
Army Reactors, DRD
U. S. Atomic Energy Commission
Washington 25, D. C. 20545
1 Copy

Defense Documentation Center
Headquarters
Cameron Station, Bldg 5
5010 Duke Street
Alexandria 4, Virginia

Attn: TISIA 1 Copy

Office, DDR and E: USW and BSS
The Pentagon
Washington 25, D. C

Attn: G. B. Wareham 1 Copy

Institute for Defense Analyses
Research and Engineering
Support Division
1666 Connecticut Avenue, N. W.
Washington 9, D. C.

Attn: Dr. George C. Szego 1 Copy

Power Information Center
University of Pennsylvania
Moore School Building
200 South 33rd Street
Philadelphia 4, Pennsylvania
1 Copy

Office of Technical Services
Department of Commerce
Washington 25, D. C. 20009 1 Copy

Battelle Memorial Institute
505 King Avenue
Columbus 1, Ohio

Attn: Dr. C. L. Faust 1 Copy

Aerojet General Corporation
Chemical Products Division
Azusa, California

Attn: Dr. S. O. Rosenberg
1 Copy

Aeronutronic Division
Philco Corporation
Ford Road
Newport Beach, California

Attn: Dr. S. W. Weller 1 Copy

Allis Chalmers Manufacturing
Company
1100 South 70th Street
Milwaukee 1, Wisconsin

Attn: Dr. Joyner 1 Copy

Arthur D. Little, Incorporated
Cambridge, Massachusetts

Attn: J. H. B. George 1 Copy

Douglas Aircraft Company, Inc.,
Astropower Laboratory
2121 Paularino Avenue
Newport Beach, California

Attn: Dr. Carl Berger 1 Copy

Atomics International Division
North American Aviation, Inc.,
Canoga Park, California

Attn: Dr. H. L. Recht 1 Copy

Electric Storage Battery Company
Carl F. Norberg Research Center
Yardley, Pennsylvania

Attn: W. S. Herbert 1 Copy

Eagle-Picher Company
Post Office Box 290
Joplin, Missouri

Attn: E. M. Morse 1 Copy

Dr. Arthur Fleischer
466 South Center Street
Orange, New Jersey 1 Copy

Electrochimica Corporation
1140 O'Brien Drive
Menlo Park, California

Attn: Dr. Morris Eisenberg
1 Copy

General Electric Corporation
Schenectady, New York

Attn: Dr. William Carson
General Engineering
Laboratory
1 Copy

Globe Union, Incorporated
900 East Keefe Avenue
Milwaukee, Wisconsin

Attn: Dr. C. K. Morehouse
1 Copy

Gould-National Batteries, Inc.,
Engineering and Research Center
2630 University Avenue S. E.
Minneapolis 14, Minnesota

Attn: J. F. Donahue 1 Copy

Gulton Industries
Alkaline Battery Division
Metuchen, New Jersey

Attn: Dr. Robert Shair 1 Copy

Hughes Research Laboratories
Corporation
Malibu, California

Attn: T. M. Hahn 1 Copy

Livingston Electronic Corporation
Route 309 opposite Springhouse Quarry
Montgomeryville, Pennsylvania

Attn: William F. Meyers
1 Copy

Lockheed Aircraft Corporation
1123 N. Mathilda Avenue
Sunnyvale, California

Attn: J. E. Chilton
1 Copy

P. R. Mallory and Company
Northwest Industrial Park
Burlington, Massachusetts

Attn: Dr. Per Bro 1 Copy

Hoffman Electronics Company
Research Laboratory
Santa Barbara, California

Attn: Dr. J. Smatko
1 Copy

Magna Corporation
Division of TRW, Incorporated
101 South East Avenue
Anaheim, California

Attn: Dr. G. Rohrbach 1 Copy

Marquardt Corporation
16555 Saticoy Street
Van Nuys, California

Attn: Dr. H. G. Krull 1 Copy

Melpar, Incorporated
3000 Arlington Boulevard
Falls Church, Virginia

Attn: Dr. R. T. Foley 1 Copy

Monsanto Research Corporation
Everett 49, Massachusetts

Attn: Dr. J. O. Smith 1 Copy

Radio Corporation of America
Somerville, New Jersey

Attn: Dr. H. S. Lozier
1 Copy

Space Technology Laboratories, Inc.,
2400 E. El Segundo Boulevard
El Segundo, California

Attn: Dr. A. Krausz 1 Copy

Southwest Research Institute
8500 Culebra Road
San Antonio 6, Texas

Attn: Dr. Jan Al 1 Copy

Power Sources Research Laboratory
Whittaker Corporation
9601 Canoga Avenue
Chatsworth, California 91311

Attn: Dr. M. Shaw 1 Copy

University of Pennsylvania
Electrochemistry Laboratory
Philadelphia 4, Pennsylvania

Attn: Prof. J. O'M. Brockris

Yardney Electric Corporation
New York, New York

Attn: Dr. Paul Howard 1 Copy

Union Carbide Corporation
Parma Research Center
Advanced Developments Department
12900 Snow Road
Parma, Ohio

Attn: Dr. R. A. Charpie 1 Copy

Westinghouse Electric Corporation
Research and Development Center
Churchill Borough
Pittsburgh, Pennsylvania

Attn: Dr. A. Langer 1 Copy

P. R. Mallory and Company, Inc.
3029 East Washington Street
Indianapolis, Indiana 46206

Attn: Technical Library
1 Copy